

# ***HST observations of the cometary blue compact dwarf galaxy UGC 4483: a relatively young galaxy?***<sup>1</sup>

Yuri I. Izotov

*Main Astronomical Observatory, National Academy of Sciences of Ukraine, 03680, Kyiv,  
Ukraine*

[izotov@mao.kiev.ua](mailto:izotov@mao.kiev.ua)

and

Trinh X. Thuan

*Astronomy Department, University of Virginia, Charlottesville, VA 22903*

[txt@virginia.edu](mailto:txt@virginia.edu)

## **ABSTRACT**

We present  $V$  and  $I$  photometry of the resolved stars in the cometary blue compact dwarf galaxy UGC 4483 using *Hubble Space Telescope* Wide Field Planetary Camera 2 (WFPC2) images. The resulting  $I$  vs.  $(V - I)$  color-magnitude diagram (CMD) reaches limiting magnitudes  $V = 27.5$  mag and  $I = 26.5$  mag for photometric errors less than 0.2 mag. It reveals not only a young stellar population of blue main-sequence stars and blue and red supergiants, but also an older evolved population of red giant and asymptotic giant branch stars. The measured magnitude  $I = 23.65 \pm 0.10$  mag of the red giant branch tip results in a distance modulus  $(m - M) = 27.63 \pm 0.12$ , corresponding to a distance of  $3.4 \pm 0.2$  Mpc. The youngest stars are associated with the bright H II region at the northern tip of the galaxy. The population of older stars is found throughout the low-surface-brightness body of the galaxy and is considerably more spread out than the young stellar population, suggesting stellar diffusion. The most striking characteristics of the CMD of UGC 4483 are the very blue colors of the red giant stars and the high luminosity of the asymptotic giant branch stars. Both of these characteristics are consistent with either: 1) a very low metallicity ( $[\text{Fe}/\text{H}] = -2.4$  like the most metal-deficient globular clusters) and an old age of 10 Gyr, or 2) a higher metallicity ( $[\text{Fe}/\text{H}] = -1.4$  as derived from the ionized gas emission lines) and a relatively young age of the oldest stellar population in UGC 4483, not exceeding  $\sim 2$  Gyr. Thus our data do not exclude the possibility that UGC 4483 is a relatively young galaxy having formed its first stars only  $\sim 2$  Gyr ago.

*Subject headings:* galaxies: irregular — galaxies: photometry — galaxies: stellar content — galaxies: distances and redshifts — galaxies: evolution — galaxies: individual (UGC 4483)

## 1. Introduction

The dwarf irregular galaxy UGC 4483 can also be classified as a cometary blue compact dwarf (BCD) galaxy in the morphological classification scheme of Loose & Thuan (1986): the high-surface-brightness starburst region at the northern end of the galaxy represents the “head” of the comet while its low-surface-brightness (LSB) elongated body represents its “tail”. With equatorial coordinates  $\alpha(\text{J2000}) = 08^{\text{h}}37^{\text{m}}03\text{:}0$ ,  $\delta(\text{J2000}) = +69^{\circ}46'31''$ , it lies roughly midway between M81 (7.8 away) and NGC 2403 (7.3 away) and likely belongs to the M81 group of galaxies. Tikhonov & Karachentsev (1993) have derived a distance to UGC 4483 of 3.6 Mpc from photometry of its brightest stars. For comparison, the Cepheid-determined distance to M81 is 3.47 Mpc and that to NGC 2403 is 2.82 Mpc. Recently Dolphin et al. (2001) using *Hubble Space Telescope* (*HST*) observations have derived a lower distance of 3.2 Mpc and have argued that UGC 4483 belongs to the NGC 2403 subgroup rather than to the M81 subgroup. From H I 21 cm observations, Thuan & Seitzer (1979) derived for UGC 4483 a radial velocity of  $+156 \text{ km s}^{-1}$ , a hydrogen mass  $M(\text{H I}) = 4.1 \times 10^7 M_{\odot}$  (at a distance of 3.4 Mpc) and a gas mass fraction of 0.39.

The first abundance determination of the ionized gas surrounding the brightest H II region on the northern side of the extended LSB body in UGC 4483 is by Skillman (1991) who derived an oxygen abundance  $12 + \log \text{O/H} = 7.32$ . However, subsequent spectroscopic studies have resulted in higher values: 7.52 (Skillman et al. 1994), 7.58 (Izotov, Thuan & Lipovetsky 1994) and 7.54 ( $Z_{\odot}/23$ ) (Izotov & Thuan 1999). This low metallicity makes UGC 4483 a good candidate for being a relatively unevolved galaxy. Its nitrogen-to-oxygen abundance ratio  $\log \text{N/O} = -1.64 \pm 0.03$  falls in the narrow range of values derived for other very metal-deficient BCDs with  $Z \leq Z_{\odot}/20$  (Thuan, Izotov & Lipovetsky 1995; Izotov & Thuan 1999). Izotov & Thuan (1999) have argued that chemical abundances in BCDs can be used to put constraints on their age. From the constancy of the C/O and N/O ratios as a function of O abundance, they have suggested that all galaxies with  $12 + \log (\text{O/H}) \lesssim 7.6$  ( $Z_{\odot}/20$ ) began to form stars less than  $\sim 100$  Myr ago. However, the most direct way

---

<sup>1</sup>Based on observations obtained with the NASA/ESA *Hubble Space Telescope* through the Space Telescope Science Institute, which is operated by AURA, Inc. under NASA contract NAS5-26555.

to derive the age of galactic stellar populations is by color-magnitude diagrams (CMD) of resolved stars and comparison with theoretical isochrones.

We report here *HST* Wide Field and Planetary Camera 2 (WFPC2) *V* and *I* imaging of UGC 4483. These data are used to discuss the evolutionary status of this nearby dwarf galaxy. We describe the observations in Sect. 2. The distance to UGC 4483 is derived in Sect. 3. Its stellar populations are discussed in Sect. 4. In Sect. 5 we compare the CMD of UGC 4483 with those of other nearby irregular and BCD galaxies available from the *HST* archives. We summarize our findings in Sect. 6.

## 2. Observations and data reduction

We obtained *HST* images of UGC 4483 on 2000 August 12 during cycle 9 with the WFPC2 through filters F555W and F814W, which we will refer to hereafter as *V* and *I*. The *V* exposure was broken up in seven sub-exposures and the *I* filter in five sub-exposures to permit identification and removal of cosmic rays. The total exposure time was 9500s in *V* and 6900s in *I*. The galaxy was positioned on the PC frame so that the high-surface-brightness starburst region is at its North corner. The orientation of the WFPC2 has been chosen so that the major axis of the galaxy lies along the diagonals of the PC and WF3 frames. Some parts of UGC 4483 were imaged also on the WF2, WF3 and WF4 frames. The scale is 0''.046 per pixel for the PC frame and 0''.102 per pixel for the WF frames.

Preliminary processing of the raw images including flat-fielding was done at the Space Telescope Science Institute through the standard pipeline. Subsequent reductions were carried out at the Main Astronomical Observatory of the Ukrainian Academy of Sciences using IRAF<sup>2</sup> and STSDAS<sup>3</sup>. Cosmic rays were removed and the images in each filter were combined using the CRREJ routine. We found that all exposures in a given filter coregistered to better than  $\sim 0.2$  pixels.

In Fig. 1 is shown the mosaic *V* image of UGC 4483. Many faint background galaxies are visible in the field, with several such galaxies along the line of sight to UGC 4483. The most prominent projected galaxy is located near the brightest star cluster. It is red, so is better seen in *I* and *V* – *I* images. In Fig. 2 we show PC *I* and *V* – *I* images where the

---

<sup>2</sup>IRAF is the Image Reduction and Analysis Facility distributed by the National Optical Astronomy Observatory, which is operated by the Association of Universities for Research in Astronomy (AURA) under cooperative agreement with the National Science Foundation (NSF).

<sup>3</sup>STSDAS: the Space Telescope Science Data Analysis System.

prominent background galaxy is marked by a circle. The dark regions in the  $V - I$  image are young regions with ongoing star formation and ionized gas emission. They have a patchy structure implying non-uniform dust extinction.

The superior spatial resolution of the *HST* WFPC2 images combined with the proximity of UGC 4483 permits to resolve individual stars and study stellar populations in this galaxy by means of CMDs. We used the DAOPHOT package in IRAF for point-spread-function (PSF) fitting photometry. The PSFs are derived using the brightest stars in each frame. There are many bright and relatively uncrowded stars in the PC frame, resulting in a reliable PSF. The PSFs for the WF frames are not as reliable because of the lack of bright isolated stars. The measured full widths at half maximum (FWHM) of the stellar profiles are different for the PC and WF frames and for different filters. For the PC frame we obtain FWHMs of 1.8 pixels and 2.3 pixels respectively for the  $V$  and  $I$  images. The corresponding FWHMs for the WF frames are 1.5 pixels and 1.7 pixels. The background level in the PC field was measured in an annulus with radii 21 and 25 pixels (0''.97 and 1''.15) around each source and subtracted. These radii are large enough so that the background annulus is free of contamination from the extended wings of the stellar profiles. We have checked that this is the case by using a background annulus closer to the source, with radii of 11 and 15 pixels (0''.51 and 0''.69). The measured magnitudes with the larger annulus are  $\lesssim 0.005$  mag brighter than those obtained with the smaller annulus, implying that the wings of the stellar profiles do not contaminate the background appreciably at radii  $> 0''.5$ . The sky level in the WF fields was measured in an annulus with radii 11 and 15 pixels (1''.12 and 1''.53). We also experimented with a smaller background annulus with radii 6 and 11 pixels (0''.61 and 1''.12) and did not find differences in the measured magnitudes, implying again that the wings of the stellar profiles do not contaminate the background for radii  $> 0''.5$ . The zero point of the PSF-fitting stellar photometry was determined with the standard aperture photometry technique adopting a 2 pixel radius aperture in all frames. To convert instrumental magnitudes with an aperture radius of 2 pixels to the corresponding magnitudes with the Holtzman et al. (1995a) calibrating aperture radius of 0''.5 (respectively 11 and 5 pixels for the PC and WF frames), we need to derive aperture corrections. For this, we compared PSF-fitted magnitudes of bright isolated stars with the magnitudes of the same stars measured with the aperture photometry technique within an 0''.5 aperture. For the PC frames we obtained the corrections  $V_{\text{ap}}(0''.5) - V_{\text{fit}} = -0.37$  mag and  $I_{\text{ap}}(0''.5) - I_{\text{fit}} = -0.60$  mag. For the WF frames the corresponding corrections are  $-0.22$  mag in  $V$  and  $-0.23$  mag in  $I$ . Our derived corrections are very similar to those obtained by Holtzman et al. (1995a).

Stars with  $\chi^2$  greater than 4.0 and a sharpness out of the  $-1.0 - +1.0$  range in both PC and WF frames were eliminated to minimize the number of false detections. Correction for charge-transfer efficiency (CTE) loss has been done according to the prescriptions of

Dolphin (2000a). Figure 3 shows the distribution of photometric errors as a function of  $V$  and  $I$  magnitudes as determined by DAOPHOT. It is seen that errors are about 0.2 mag at  $V = 27.5$  mag and  $I = 26.5$  mag for both PC and WF frames. They increase to about 0.4 mag at  $V = 28.5$  mag and  $I = 27.5$  mag.

We have excluded stars with photometric errors larger than 0.2 mag in the final photometric list for both  $V$  and  $I$  images. The total numbers of recovered stars in both PC and WF frames are respectively 7672, 5411 and 3853 in the  $V$  image, the  $I$  image and in both of these images at the same time. The corresponding numbers of recovered stars in the PC frame only are 4508, 2985 and 2250. We have adopted a matching radius of 1 pixel, although changing that radius within the range 0.5 - 2 pixels does not change the number of stars in both  $V$  and  $I$  frames appreciably. That nearly half the stars are not matched is likely to be caused by incompleteness effect and an increasing number of false detections at faint magnitudes. Indeed, the number of the stars with  $V = 25 - 26$  mag recovered in both  $V$  and  $I$  images is  $\sim 85\%$  that recovered in the  $V$  image alone, while the number of the stars with  $V = 27 - 28$  mag recovered in both  $V$  and  $I$  images is only  $\sim 15\%$  that recovered in the  $V$  image alone.

The transformation of instrumental magnitudes to the Johnson-Cousins  $UBVRI$  photometric system as defined by Landolt (1992) was performed according to the prescriptions of Holtzman et al. (1995b) and Dolphin (2000a). The magnitudes and colors of point sources were corrected for Galactic interstellar extinction adopting  $A_V = 0.11$  mag (Schlegel, Finkbeiner & Davis 1998).

We have carried out a completeness analysis for the PC and WF4 frames using the DAOPHOT routine ADDSTAR. For each frame we have added artificial stars amounting to  $\sim 5\%$  of the real stars detected in each magnitude bin in the original image. We then performed a new photometric reduction using the same procedure as the one applied to the original frame, and checked how many added stars were recovered. This operation was repeated 10 times for each frame and each magnitude bin and the results were averaged. The completeness factor in each magnitude bin defined as the percentage of recovered artificial stars is shown in Table 1. It can be seen that the completeness limit is reasonably good: it is about 67% – 70% in  $V$  and 45% – 55% in  $I$  in the 26 – 27 mag range, but drops to  $\sim 41\%$  – 44% and  $\sim 7\%$  – 15% in the 27 – 28 mag range.

### 3. Distance determination

In Fig. 4 we show  $I_0$  vs  $(V - I)_0$  CMDs of UGC 4483 in all WFPC2 frames. The CMD for the PC frame is well populated by both young main sequence stars and older red giant branch (RGB) and asymptotic giant branch (AGB) stars. Such populations have also been detected and discussed by Dolphin et al. (2001) from less deep  $V$  and  $I$  *HST*/WFPC2 images. The CMDs in the WF frames are less populated, with a dominant contribution from RGB and AGB stars, although younger stellar populations are present.

The detection of RGB stars allows in principle to derive the distance to the galaxy using the apparent magnitude  $I_0$  of the tip of RGB stars (TRGB). This technique is based on the observed constancy of the absolute magnitude  $M_{I0} \approx -4.0$  mag of TRGB stars in old globular stellar clusters (Da Costa & Armandroff 1990). There is evidently a sharp drop in the RGB distribution toward brighter  $I_0$  magnitudes in the PC, WF2 and WF3 frames (Fig. 4a – 4c). However the drop is not so evident in the WF4 frame (Fig. 4d) because of the large number of AGB stars atop the RGB tip. Therefore, care has been taken to minimize the contribution of AGB stars and more massive red helium burning (RHeB) stars in the determination of  $I_0$ (TRGB). For all frames, we have derived the distribution of the RGB stars located in the CMD to the red of the straight line defined by the pair of points  $I_0, (V - I)_0 = (27, 0.4)$  and  $(22, 1.5)$  to exclude the contribution of the RHeB stars, and to the blue of the straight line defined by  $I_0, (V - I)_0 = (27, 0.8)$  and  $(22, 1.9)$  to reduce the contribution of the AGB stars.

The distribution of stars in the combined PC, WF2, WF3, WF4 frames in steps  $\Delta I_0 = 0.1$  mag is shown in Fig. 5 by a solid line. The derivative of the distribution is shown by a dotted line. The location of the TRGB is determined by the first large increase in both the RGB luminosity function and its derivative, and is shown by a vertical tick mark. The  $I_0$ (TRGB) is  $23.65 \pm 0.10$  mag. We also experimented with luminosity functions produced with different binnings,  $\Delta I_0 = 0.2$  and  $0.4$  mag. The larger  $\Delta I_0$  result in more monotonic luminosity functions, but the value of the  $I_0$ (TRGB) is unchanged. It is 0.09 mag fainter, but is consistent within the errors with the one of  $23.56 \pm 0.10$  mag derived by Dolphin et al. (2001) from their short-exposure WF observations.

The distance modulus is given by  $(m - M)_I = I_0(\text{TRGB}) - M_{I0}(\text{TRGB})$  with the absolute  $I$  magnitude defined as  $M_{I0}(\text{TRGB}) = M_{\text{bol}}(\text{TRGB}) - BC(I)$ , where  $M_{\text{bol}}(\text{TRGB})$  is the bolometric magnitude of the TRGB and  $BC(I)$  is the bolometric correction to the  $I$  magnitude.  $BC(I)$  is related to the  $(V - I)$  color of the TRGB by  $BC(I) = 0.881 - 0.243(V - I)_{\text{TRGB}}$ , while the bolometric magnitude is related to the stellar metallicity  $[\text{Fe}/\text{H}]$  by  $M_{\text{bol}}(\text{TRGB}) = -0.19[\text{Fe}/\text{H}] - 3.81$  (Da Costa & Armandroff 1990; Lee, Freedman & Madore 1993). Usually  $[\text{Fe}/\text{H}]$  is derived using the  $(V - I)$  color of RGB stars with absolute magnitude  $M_{I0} = -3$ . As pointed out by Lee et al. (1993) from analysis of Yale theoretical

isochrones, this is because  $(V - I)$  is mainly dependent on metallicity and not very much on age. We caution however that this method for estimating metallicities of RGB stars may be less reliable when applied to relatively young stellar populations like those in UGC 4483 (see section 4.2), because Lee et al. (1993) have restricted their analysis to stellar ages larger than 7 Gyr. Furthermore, the Yale isochrones do not give a good fit to the observed isochrones for globular clusters (see the discussion by Da Costa & Armandroff 1990).

Fig. 6a shows the RGB region as obtained from the PC frame. We adopt a distance modulus  $m - M = 27.63$ , as discussed later. The superimposed solid lines are, in order of increasing metallicity from left to right, the observed isochrones of the Galactic globular clusters M15, NGC 6397, M2, NGC 6752, NGC 1851 and 47 Tuc with respective metallicities  $[\text{Fe}/\text{H}] = -2.17, -1.91, -1.58, -1.54, -1.29$  and  $-0.71$  (Da Costa & Armandroff 1990). Fig. 6b shows the RGB region of the combined CMD for the WF2, WF3 and WF4 frames.

It is seen from Fig. 6a that the  $(V - I)$  colors of the RGB stars in UGC 4483 are  $\sim 0.1$  mag bluer as compared to those in the most metal-deficient globular cluster M15 ( $[\text{Fe}/\text{H}] = -2.17$ ) in the Da Costa & Armandroff (1990) sample. For the TRGB, we derive  $(V - I) \approx 1.3$  mag, or  $\sim 0.1$  mag bluer than in the Local Group irregular galaxy Leo A, suggested by Tolstoy et al. (1998) to contain a predominantly young stellar population. The  $(V - I)$  color of the RGB stars at  $M_{I0} = -3$  mag is  $\sim 1.1$  mag. These blue colors may result from both metallicity and age effects. Assuming that metallicity is the dominant effect we derive  $[\text{Fe}/\text{H}] = -2.39$ , using the equation  $[\text{Fe}/\text{H}] = -15.16 + 17.0(V - I)_{-3} - 4.9(V - I)_{-3}^2$ , where  $(V - I)_{-3}$  is the color of RGB stars with  $M_{I0} = -3$  mag (Da Costa & Armandroff 1990). The color-derived metallicity of the RGB stars in UGC 4483 is  $\sim 1.0$  dex lower than the one derived in the H II region. We caution however that this relation has been obtained for metallicities in the range  $-2.1 < [\text{Fe}/\text{H}] < -0.7$ , so that extrapolation to lower metallicities might be uncertain. For the metallicities  $-2.39$  and  $-1.4$  (the metallicity of the ionized gas),  $M_{I0}(\text{TRGB}) = -3.93$  and  $-4.03$  mag respectively. Then the respective distance moduli are  $(m - M) = 27.58$  and  $27.68$ . Both values are slightly larger, but not significantly, than the value of  $27.53$  derived by Dolphin et al. (2001). We adopt  $(m - M) = 27.63 \pm 0.12$ , as the mean of the two determinations. The distance to UGC 4483 is then  $D = 3.4 \pm 0.2$  Mpc, which agrees within the errors with the distance of  $3.2 \pm 0.2$  Mpc obtained by Dolphin et al. (2001).

The above distance determination is based on the assumption that the RGB stars in UGC 4483 are  $\sim 10$  Gyr old. If they are younger, the above method breaks down, and the metallicity of the RGB stars can be considerably larger. Then, theoretical isochrones should be considered to determine ages. Padua and Geneva evolutionary tracks are most often used for the analysis of resolved stellar populations in Local Group and more distant

galaxies. However, as discussed e.g., Da Costa & Armandroff (1990) and Lynds et al. (1998) the theoretical isochrones do not fit the observed ones for globular clusters. We thus need to check the applicability of the theoretical isochrones for the analysis of the RGB population. For that purpose, we compare theoretical 10 Gyr isochrones as calculated by the Padua and Geneva groups for different metallicities with those observed for galactic globular clusters.

In Fig. 7 we show theoretical isochrones for two values of the heavy element mass fraction  $Z = 0.0004$  and  $Z = 0.001$  (Bertelli et al. 1994 (Padua); Lejeune & Schaerer 2001 (Geneva)) (thin solid lines) with the observed isochrones from Da Costa & Armandroff (1990) for the globular clusters M2 with  $Z = 0.0004$  and NGC 1851 with  $Z = 0.001$  (thick solid lines). All isochrones are plotted using a distance modulus  $(m - M) = 27.63$  to fit the CMD of UGC 4483. It is seen from Fig. 7a and 7c that the 10 Gyr theoretical isochrones with  $Z = 0.0004$  from either group do not fit the observed ones. The Padua 10 Gyr isochrone is significantly bluer than the M2 isochrone, leading to a large age overestimate. Thus, the Padua isochrones would give an age of 10 Gyr for the RGB stars in UGC 4483, and an age larger than the age of the universe for M2. By contrast, the Geneva 10 Gyr isochrone is redder than that of M2, resulting in an underestimate of the age. In this case, a good fit to the RGB stars in UGC 4483 is given by the  $\sim 2$  Gyr isochrone, and the age of M2 would be 3 billion years.

The situation is better for models with  $Z = 0.001$  (Fig. 7b and 7d). Both Padua and Geneva 10 Gyr isochrones fit the observed isochrone of NGC 1851 quite well, the fit being slightly better for the Padua isochrones. However, we note that the isochrones for  $Z = 0.001$  of Bertelli et al. (1994) are based on evolutionary tracks calculated with an older set of opacities. All other isochrones with different  $Z$  given by those authors are calculated with new opacities. Girardi et al. (2000) have also computed isochrones for  $Z = 0.001$  with the new opacities. The 10 Gyr isochrones from Girardi et al. (2000) do not fit the NGC 1851 isochrone, being significantly bluer and resulting in a large age overestimate.

Evidently, the uncertainties in theoretical isochrones for ages  $\gtrsim 1$  Gyr are large, and additional work is needed. We decided to adopt  $(m - M) = 27.63 \pm 0.12$  for UGC 4483, derived from  $M_{I0}(\text{TRGB})$  in globular clusters, assuming that it does not change appreciably between 1 and 10 Gyr. Although the distance of  $3.4 \pm 0.2$  Mpc is not derived entirely in a self-consistent manner, because of the age-metallicity ambiguity, it is the best that can be done with current observations and models.

#### 4. Stellar populations

Several generations of stellar populations are present in the CMD of UGC 4483 suggesting continuous star formation over an extended period of time. Ongoing star formation is evidenced by the presence of the high-surface-brightness supergiant H II region at the northern edge of the galaxy. Past star formation is implied by the older stellar populations distributed over its whole low-surface-brightness body. In the CMD resulting from the combination of both PC and WF data (Fig. 8), we have delimited the regions occupied by the different stellar populations: the main-sequence (MS) stars with age less than  $\sim 15$  Myr, the blue loop (BL) and the red supergiant (RSG) stars with age between  $\sim 20$  Myr and  $\sim 200$  Myr, and the older AGB and RGB stars with age  $\gtrsim 1$  Gyr.

The spatial distributions of these different stellar populations are shown in Fig. 9. The main sequence stars (Fig. 9a) are nearly all located in the H II regions at the northern edge of the BCD and show a clumpy distribution. The BL/RSG stars are found in and between the H II regions and their distribution is smoother and more extended than that of the MS stars (Fig. 9b). Finally, AGB and RGB stars occupy the largest area of the galaxy (Fig. 9c – 9d). Similar results with somewhat smoother and more extended spatial distributions of populations with different ages have also been found by Dolphin et al. (2001). Such a general trend of more extended spatial distributions for older stellar populations is also found in other dwarf galaxies observed with *HST* (e.g., Lynds et al. 1998; Schulte-Ladbeck et al. 1998; Crone et al. 2000) and is likely a consequence of the diffusion and relaxation of stellar ensembles. We discuss next in detail the different stellar populations in UGC 4483.

##### 4.1. Young stellar populations

We restrict our discussion in this section to the PC image because most of the ongoing and recent star formation is concentrated there, as evidenced by the bright supergiant H II region (Fig. 1) and its blue ( $V - I$ ) color (Fig. 2b). Fig. 10 displays a zoom of the PC  $V$  and  $I$  images showing the ionizing compact stellar cluster in the supergiant H II region. The stellar cluster has a diameter  $< 1''$  or  $< 16.5$  pc for our derived distance of 3.4 Mpc. Dolphin et al. (2001) have constructed a CMD for this cluster and derived an age of 15 Myr for it. This age can not be correct, because with such an age the expected equivalent width of the H $\beta$  emission line in the H II region is less than 10Å (e.g., Schaerer & Vacca 1998), instead of the value of 169Å measured by Izotov et al. (1994). The latter value gives an age of only 4 Myr. A similar H $\beta$  equivalent width has been obtained by Skillman et al. (1994).

We measure the  $V$  and  $I$  magnitudes for this cluster using a square aperture of 27 pixels

(or  $1''.2$ ) on a side centered at the point with coordinates  $x = 601$  and  $y = 581$ , where the origin  $x = y = 0$  is at the left lower corner of the PC chip. The galaxy background, measured at several points  $\sim 3''$  away from the cluster and amounting to  $350 \text{ e}^- \text{ pixel}^{-1}$  in  $V$  and  $140 \text{ e}^- \text{ pixel}^{-1}$  in  $I$ , has been subtracted. We derive  $V = 19.38 \pm 0.01 \text{ mag}$ ,  $I = 19.61 \pm 0.01 \text{ mag}$ , and  $(V - I) = -0.23 \pm 0.01 \text{ mag}$  for the cluster. Such a blue color is typical for young ionizing stellar clusters. We have not corrected the magnitudes and colors for the contamination of the ionized gas because a precise knowledge from spectroscopic observations of the emission line intensities in exactly the same region is required. The apparent  $I$  magnitude of the cluster translates into an absolute magnitude of  $\sim -8.0 \text{ mag}$ , equivalent to the emission of  $\sim 15$  O stars with absolute magnitude  $M_I = -5 \text{ mag}$ . Approximately such a number of stars can be seen in the cluster (Fig. 10).

A very blue compact source with coordinates  $x = 625$  and  $y = 491$  is seen at a distance  $\sim 4''$  from the cluster (within the circle in Fig. 10). It is embedded within the ionized gas envelope surrounding the cluster. This source was not recovered by DAOPHOT because of its large FWHM of 4.2 pixels, about two times the FWHM of point sources. Using APPHOT and a 5-pixel aperture, we obtain  $V = 21.83 \pm 0.01 \text{ mag}$ ,  $I = 22.38 \pm 0.02 \text{ mag}$  and  $V - I = -0.55 \pm 0.02 \text{ mag}$ . With a smaller 3-pixel aperture, the respective values are  $V = 22.33 \pm 0.02 \text{ mag}$ ,  $I = 22.92 \pm 0.03 \text{ mag}$  and  $V - I = -0.59 \pm 0.04 \text{ mag}$ . Adopting the latter values, the absolute  $I$  magnitude of the source is  $-4.7 \text{ mag}$ . Its  $(V - I)$  color is bluer than the color of the most massive main-sequence O stars ( $\sim -0.3 \text{ mag}$ ). It is probably an early-type Wolf-Rayet star embedded in a H II region with a 4-pixel radius, or  $0''.18$ , corresponding to a linear radius of 3 pc. Several other bright blue stars are seen around the cluster (compare Fig. 10a and 10b). However, no appreciable ionized gas emission is present in the vicinity of these stars, and they are probably late O or early B supergiant stars.

To study the spatial variations of the stellar populations in the PC frame, we have divided it into six regions as shown in Fig. 11. Region 1 includes the supergiant H II region and contains many bright main-sequence stars as is evident from examination of its CMD in Fig. 12a. In Fig. 12, superimposed on the data are shown theoretical isochrones for  $Z = 0.001$  (Bertelli et al. 1994). We use this isochrone set because its metallicity is close to the one observed in the H II region, and its 10 Gyr isochrone fits well the observed isochrone of the globular cluster NGC 1851 which has a similar metallicity (Fig. 7b). However, as discussed in section 3, it must be kept in mind that the absolute age calibration of these isochrones is somewhat uncertain, and they are best used in a differential manner to compare stellar population ages in different regions. The logarithms of the age of each isochrone are given in Fig. 12f. Older stars are present in region 1 as well. The presence of blue loop and red supergiant stars indicates that star formation has continued in this region for the last several 100 Myr. Finally,  $\sim 2$  Gyr red giant stars can also be seen in the CMD of region

1. However, no AGB stars are seen. We conclude that, in addition to a strong recent burst of star formation as evidenced by the presence of the supergiant H II region, star formation has occurred during at least the last 2 Gyr in region 1. Alternatively, if the metallicity of the stars is significantly lower than that of the gas, then our age estimates could be significantly larger.

Similar conclusions regarding the star formation history can be made for regions 2 to 5 (Fig. 12b – 12e), except that the main sequence is not as well populated as in region 1, and ionizing upper main sequence stars are absent.

In summary, a large part of the galaxy around the supergiant H II region shows evidence for continuous star formation during at least the last 2 Gyr. The exception is region 6 which is characterized by a low density of stars, and where mainly  $\gtrsim 2$  Gyr RGB stars are present. It is likely that star formation never occurred in this region and the RGB stars migrated there from denser regions of the galaxy.

#### 4.2. The RGB and AGB stellar populations

RGB and AGB stars are good tracers of the star formation history of UGC 4483 during the last several hundred Myr (AGB stars) to  $\gtrsim 2$  Gyr (RGB stars). If there are no older stellar populations in the galaxy, then it can be considered as a relatively young galaxy, since a 2 Gyr age is much lower than the age of the Universe. Unfortunately, the galaxy is too far away for *HST* to detect the red giant clump and horizontal-branch stars which are good indicators of stellar populations older than several Gyr. Therefore, our discussion of the age of UGC 4483 will have to rely on the observed RGB and AGB stellar populations. It will be by necessity more qualitative than quantitative. This is because of the age-metallicity degeneracy of RGB star colors, the poor knowledge of the properties of AGB stars and the uncertainties in the theoretical isochrones.

We have already pointed out that the most striking feature in the CMD of UGC 4483 is that the RGB stars are very blue. The  $(V - I)$  color of the TRGB as measured in the PC frame is only 1.3 mag (Fig. 6a), bluer than the color of the TRGB of old Galactic globular clusters ( $\gtrsim 1.4$  mag). The  $(V - I)$  color of the TRGB in the WF frames, though slightly redder, is 1.35 mag, or 0.05 mag bluer than the TRGB color of the globular cluster M15 with metallicity  $[\text{Fe}/\text{H}] = -2.17$ . Such blue colors of the RGB stars can be explained in two ways: 1) by a very low metallicity  $[\text{Fe}/\text{H}] \sim -2.4$  and an old age, or 2) by a higher metallicity and a younger age ( $< 10$  Gyr).

Let's first consider case 1. If we suppose that the RGB stars in UGC 4483 are 10 Gyr

old, then the extremely low metallicity required to produce their relatively blue colors is not easily understood. While stars with  $[\text{Fe}/\text{H}] \sim -2.4$  cannot be excluded in principle, they are rare in the Milky Way and in other well-studied nearby galaxies. There is an additional problem: if the slightly redder colors of the RGB stars seen in the WF frames is a real effect due to a higher metallicity, why would stars seen in the periphery of UGC 4483 which are likely to be older be more metal-rich as compared to the younger RGB stars in the main body of the galaxy? It is more plausible that case 2 prevails, that the blue colors of the RGB stars in UGC 4483 are caused by their younger age rather than by their lower metallicity. In that case, the metallicity of the ionized gas, while being probably higher than the stellar metallicity, may still be a reasonable approximation for the metallicity of the RGB stars. Then, using models with  $Z = 0.001$  from Bertelli et al. (1994), we derive an age for the RGB stars of  $\sim 2$  Gyr. Uncertainties in the theoretical isochrones and the unknown metallicity of the RGB stars in UGC 4483 preclude a more precise determination. While our CMDs do not show evidence for stellar populations older than  $\sim 2$  Gyr, they do not go deep enough to definitively rule them out.

AGB stars are tracers of the intermediate and old stellar populations. They are not as numerous in UGC 4483 as, for example, in the BCD VII Zw 403 (see Fig. 9 in Lynds et al. 1998) which has a slightly higher ionized gas metallicity ( $Z \sim Z_{\odot}/15$ ). AGB stars in UGC 4483 have a mean absolute  $I$  magnitude  $\sim -4.9$  mag (Fig. 6a and 6b) and are brighter by  $\sim 0.3$  mag than those in VII Zw 403 and UGCA 290 (Fig. 6c and 6d). Again, as in the case of RGB stars, the difference in the absolute brightness of the AGB stars in UGC 4483 can be due to two reasons: a lower metallicity and/or a younger age than in VII Zw 403 and UGCA 290.

There are no theoretical isochrones that can reproduce well the observed properties of AGB stars at low metallicities (e.g., Lynds et al. 1998). While AGB stars in the CMDs of UGC 4483, VII Zw 403 and some Local Group irregular galaxies have a constant absolute magnitude  $M_I$ , the models predict a steady increase of  $M_I$  with increasing  $(V - I)$  color, to the tip of the AGB (TAGB) phase, when the brightness of AGB stars reaches their maximum. The Padua theoretical isochrones with  $Z < 0.001$  are too short and too steep to be able to reproduce the red colors of AGB stars (e.g., Fig. 7a – 7b). As for Geneva isochrones, they do not include the AGB stage. Therefore, instead of performing an absolute comparison of the theoretical isochrones with the data points we can only perform a qualitative differential comparison of the AGB populations seen in UGC 4483 and VII Zw 403, using the Bertelli et al. (1994)  $Z = 0.001$  models. Assuming that the AGB stars in both galaxies have the same metallicity, the difference of 0.3 mag in the TAGB brightness translates into two times younger age for the AGB stars in UGC 4483. Again, as in the case of the RGB stars, we find that the stellar populations seen in UGC 4483 are likely not to be older than  $\sim 2$  Gyr,

an age which is considerably smaller than the age of the universe and which suggests that UGC 4483 is probably a relatively young galaxy as compared to other dwarf galaxies.

### 4.3. Surface-brightness and color distributions

Another way to study the properties of stellar populations is to consider their integrated characteristics as given by the surface brightness and color profiles in different regions in the galaxy. The advantage of this approach is that it includes both resolved and unresolved stars. The disadvantage is that populations with different ages contribute to the integrated light and assumptions have to be made on the star formation history to derive the age distribution of stars.

In Fig. 13, we show the  $V$  (a) and  $I$  (b) surface-brightness and  $V - I$  (c) color distributions along the major axis of UGC 4483 in a strip  $2''$  wide centered on the H II region taken to be the origin. As before, surface brightnesses and colors have been transformed to the standard  $VI$  photometric system according to the prescriptions of Holtzman et al. (1995b) and have been corrected for Galactic extinction with  $A_V = 0.11$  mag (Schlegel et al. 1998). The red background galaxy to the north of the H II region seen in Fig. 2 is labeled B.G. in Fig. 13b. Its peak ( $V - I$ ) color exceeds 1.0 mag (Fig. 13c). The gap in Fig. 13 at the distance of  $\sim -35''$  is caused by the lack of signal at the boundaries of the individual CCD chips (Fig. 1). The supergiant H II region has a peak surface brightness  $\mu(V) \sim 20.0$  mag  $\text{arcsec}^{-2}$ , or  $\sim 2$  mag brighter than the surrounding regions. Its profile is broader in  $V$  (Fig. 13a) than in  $I$  (Fig. 13b) because of the larger contribution of the extended ionized gas emission in  $V$ . Therefore, the region with blue ( $V - I$ ) color is very broad (Fig. 13). The bluest color in this region is  $\sim -0.3$  mag, bluer than the  $-0.23$  mag color derived for the central ionizing cluster. The difference comes from the fact that some ionized gas emission around the cluster was subtracted in the derivation of the cluster color, while Fig. 13 shows the total stellar and gaseous emission.

Fig. 13c shows an evident ( $V - I$ ) color gradient. The bluer colors for distances between  $-20''$  and 0 suggest the presence of young stellar populations, while the asymptotic value of  $(V - I) \sim 0.7$  mag attained for distances between  $-60''$  and  $-40''$  is characteristic of evolved RGB and AGB stellar populations (see the CMD in Fig. 4c and spatial distributions in Fig. 9). This ( $V - I$ ) color is slightly bluer (by  $\sim 0.1$  mag) than the one predicted for a  $\sim 2$  Gyr single stellar population by the Padua models with  $Z = 0.0004$  and  $0.001$  (Tantalo et al. 1996; Girardi et al. 2000; <http://pleiadi.pd.astro.it>). A 10 Gyr population would have a predicted  $(V - I) \sim 0.9 - 1.0$  mag, which is evidently not the case for UGC 4483. The combination of a 2 Gyr and older stellar populations, such as produced by constant star

formation between 2 Gyr and 10 Gyr ago, would result in a redder color than observed.

We now compare the asymptotic value of  $(V - I)$  with the integrated colors of the globular clusters considered before in section 3. From the catalogue of Galactic globular clusters of Harris (1996) we obtained extinction-corrected  $(V - I)$  of 0.72, 0.80, 0.84, 0.88, 0.98 and 1.09 mag respectively for the M15, NGC 6397, M2, NGC 6752, NGC 1851 and 47 Tuc clusters, arranged in order of increasing metallicity. It can be seen that while the observed asymptotic color of 0.7 mag in UGC 4483 is consistent with that of a 10 Gyr population with the metallicity  $[\text{Fe}/\text{H}] = -2.17$  of M15, the colors of the other clusters with higher metallicities are too red. Therefore, if the metallicity of the stars in UGC 4483 is larger than that of M15 then we again conclude that their age is younger than that of globular clusters. It is interesting to note that in spite of the Padua 10 Gyr theoretical isochrones being bluer than those observed for globular clusters, the predicted colors of single stellar populations are redder than the integrated colors of globular clusters. This is likely due to the steepness of the theoretical isochrones which results in too large predicted luminosities for the AGB stars.

A relatively young age seems to be typical of cometary galaxies. Thuan, Izotov & Foltz (1999) found the age of the stellar populations in the cometary BCD SBS 1415+437 ( $Z_\odot/21$ ) to be less than  $\sim 100$  Myr. Although the latter age is probably an underestimate because it was derived using instantaneous burst rather than continuous star formation models, the very blue  $V - I$  of  $\sim 0.4$  mag of its extended LSB body argues for an age less than 1 Gyr. Noeske et al. (2000) found in a detailed study of two less metal-deficient cometary BCDs, Mrk 71 ( $Z_\odot/14$ ) and Mrk 59 ( $Z_\odot/8$ ), that their stellar populations are not older than  $\sim 3$  Gyr in the first one, and  $\sim 4$  Gyr in the second one. On the basis of this very small sample, there may be a trend of younger age with lower metallicity, although a larger sample is needed to really tell.

Our age estimate of  $\sim 2$  Gyr for UGC 4483 is larger than the age of  $\lesssim 100$  Myr suggested by Izotov & Thuan (1999) for the class of very-metal deficient galaxies with  $Z \lesssim 1/20 Z_\odot$ , to which UGC 4483 belongs. Their argument is based on the observed constancy of the N/O and C/O ratios with O/H. Izotov & Thuan (1999) argued that the constancy meant that carbon and nitrogen in these metal-deficient galaxies are made by the same massive stars responsible for oxygen production. In other words, intermediate-mass ( $3M_\odot \lesssim M \lesssim 9M_\odot$ ) stars have not had the time to release their nucleosynthetic products, which puts an upper limit of  $\lesssim 40$  Myr, the main-sequence lifetime of a  $9M_\odot$  star. However, there are several reasons to believe that the above age upper limit is too low. First, the major nitrogen production is not by  $8M_\odot$  stars, but by  $3 - 4M_\odot$  stars (e.g., Marigo 2001), increasing the time-scale for nitrogen enrichment of the interstellar medium by intermediate-mass stars to at least to  $\sim$

150 – 400 Myr. Second, some additional time of  $\lesssim 1$  Gyr (Roy & Kunth 1995) should be allowed for the mixing of fresh nitrogen to the interstellar medium. Other possibilities can be considered for reconciling the chemical abundance considerations with the age of UGC 4483. One possible way out is to note that chemical evolution models of dwarf galaxies follow the time evolution of local characteristics or assume instantaneous recycling of the matter. In particular, in closed-box models both oxygen and nitrogen are produced at the same place. However, judging from the spatial distribution of main-sequence stars and AGB stars in UGC 4483 (Fig. 9), this assumption may not be hold for this galaxy. The massive main sequence stars which are the main contributors to the interstellar medium of oxygen and probably of primary nitrogen (Izotov & Thuan 1999) are located in very compact regions of the galaxy, while the AGB stars occupy a much larger volume. This may result in a volume dilution of the nitrogen produced by AGB stars as compared to the oxygen and primary nitrogen produced by massive stars, decreasing the relative contribution of nitrogen by AGB stars. Other scenarios of nitrogen enrichment have been discussed, but they cannot account for the very small dispersion of the N/O and C/O ratios in very metal-deficient galaxies and the increase in scatter of those ratios in higher-metallicity galaxies (e.g., Pilyugin 1999; Henry, Edmunds & Köppen 2000).

We note also that the asymptotic  $V - I$  of  $\sim 0.7$  of UGC 4483 is the reddest color of all values derived thus far in our long-term study of the stellar populations in extremely metal-deficient BCDs, those with  $Z \lesssim Z_{\odot}/20$  (Izotov & Thuan 1999). The  $V - I$  asymptotic colors of I Zw 18 ( $Z_{\odot}/50$ ), SBS 0335–052 ( $Z_{\odot}/41$ ), SBS 0940+544 ( $Z_{\odot}/28$ ) and SBS 1415+437 ( $Z_{\odot}/21$ ) are respectively 0 (Papaderos et al. 2001), 0 (Thuan, Izotov & Lipovetsky 1997), 0.6 (Guseva et al. 2001) and 0.4 (Thuan et al. 1999). The colors of I Zw 18 and SBS 0335–052 are extremely blue, partly because the contribution of ionized gas emission is very important, even at large distances from the main star-forming regions. The ages derived for the oldest stellar populations in the above BCDs are all  $\lesssim 1$  Gyr, so that the age of  $\sim 2$  Gyr derived here from our CMD analysis of UGC 4483 is consistent with the idea that redder  $V - I$  colors are caused mainly by age rather than metallicity effects.

## 5. Comparison with CMDs of other galaxies

There has been several studies of the resolved stellar populations and star formation histories in Local Group and other nearby galaxies based on *HST* WFPC2 observations during the last few years. To put our findings in perspective, we have compared the CMD of UGC 4483 with those of several dwarf galaxies observed by *HST* with the same F555W and F814W filters and for which data are available in the archives. Our aim was to produce

a homogeneous set of CMDs of dwarf galaxies reduced in the same manner so as to detect possible general trends. We have constructed the CMDs of three BCDs, I Zw 18 with an ionized gas metallicity  $Z_{\odot}/50$  (Hunter & Thronson 1995; Aloisi, Tosi & Gregg 1999), VII Zw 403 ( $Z_{\odot}/15$ , Lynds et al. 1998; Schulte-Ladbeck et al. 1998), UGCA 290 (Crone et al. 2000), of the dwarf irregular galaxy NGC 2366 ( $Z_{\odot}/14$ , Thuan & Izotov 2001) and of six Local Group dwarf irregular galaxies, IC 1613 ( $Z_{\odot}/13$ , Cole et al. 1999), NGC 6822 ( $Z_{\odot}/5$ , Wyder, Hodge & Zucker 2000), WLM ( $Z_{\odot}/15$ , Dolphin 2000b), Pegasus ( $Z_{\odot}/10$ , Gallagher et al. 1998), Sextans A ( $Z_{\odot}/27$ , Dohm-Palmer et al. 1997a, 1997b) and Leo A ( $Z_{\odot}/26$ , Tolstoy et al. 1998).

In Fig. 14, we show the CMDs for UGC 4483 separately for the PC and WF frames, along with those for the other 10 dwarf galaxies. The CMD of I Zw 18 was based only on PC data, and that for Leo A based on WF3 and WF4 data. The CMDs for the other galaxies are based on all four frames of the WFPC2. We adopt distance moduli  $(m - M) = 27.63$  for UGC 4483, 28.25 for VII Zw 403 (Lynds et al. 1998), 29.1 for UGCA 290 (Crone et al. 2000), 27.6 for NGC 2366 (Thuan & Izotov 2001), 24.27 for IC 1613 (Cole et al. 1999), 23.69 for NGC 6822 (Wyder et al. 2000) 24.88 for WLM (Dolphin 2000b), 24.4 for Pegasus (Gallagher et al. 1998), 25.8 for Sextans A (Dohm-Palmer et al. 1997a) and 24.2 for Leo A (Tolstoy et al. 1998). All CMDs have been corrected for extinction as quoted in the above mentioned papers. The only galaxy in Fig. 14 where the RGB population is not detected and hence the distance not constrained, is I Zw 18, the BCD with the lowest metallicity known. We adopt for it a distance modulus  $(m - M) = 31.0$  and correct its magnitudes and colors for a small Galactic extinction with  $E(B - V) = 0.032$  mag (Schlegel et al. 1998). The adopted distance modulus for I Zw 18 corresponds to a distance of 15.8 Mpc, larger than the redshift distance of 10.8 Mpc adopted by Hunter & Thronson (1995) and Aloisi et al. (1999), and that of 12.6 Mpc used by Östlin (2000). The larger distance adopted by us is based on the plausible assumption that the brightest stars in the CMD of I Zw 18 have absolute  $I$  magnitudes in the same range as those of the brightest stars in the CMDs of UGC 4483, VII Zw 403, UGCA 290 and NGC 2366 which are also undergoing active star formation, i.e. between –8 mag and –9 mag. For distances of 10.8 Mpc and 12.6 Mpc, the absolute magnitudes of the brightest stars in the I Zw 18 CMD would be 0.83 mag to 0.5 mag fainter, which is hard to understand. For comparison, we also show in Fig. 14 the observed isochrones for the two Galactic globular clusters M15 and NGC 1851 with respective metallicities  $[\text{Fe}/\text{H}] = -2.17$  and –1.29 (Da Costa & Armandroff 1990).

It is evident from Fig. 14a – 14b that the RGB stars in UGC 4483 are the bluest as compared to those in other galaxies, supporting the conclusion that UGC 4483 may be the youngest among the considered galaxies, except for I Zw 18 where the RGB stellar population is not seen. A very similar age of 1 – 2 Gyr has been derived by Tolstoy et al. (1998) for

the oldest stars of Leo A. They also concluded that this galaxy is relatively young. We note however that the AGB stars in Leo A (Fig. 14l) are fainter than those in UGC 4483, implying that they have a larger age or alternatively, a larger metallicity. In other Local Group galaxies (Fig. 14g – 14k), red giant clump and/or horizontal-branch stars and RR Lyr variables imply the presence of a several Gyr old stellar population. The detection of such stars is not possible with *HST* for galaxies beyond the Local Group. However, comparing the CMD of UGC 4483 (Fig. 14a – 14b) with those of the dwarf galaxies VII Zw 403, UGCA 290 and NGC 2366 (Fig. 14c – 14e), we conclude that the RGB and AGB stars in the latter galaxies are likely to be older, the RGB stars because their mean color is redder and the AGB stars because their mean luminosity is lower. We have shown in detail the CMDs of VII Zw 403 and UGCA 290 respectively in Figures 6c and 6d. It can be clearly seen that the RGB tip in UGC 4483 is bluer by  $\sim 0.2$  mag and its AGB stars are brighter by  $\sim 0.3$  mag than their counterparts in VII Zw 403 and UGCA 290. According to Bertelli et al. (1994), this would mean that the AGB stars in UGC 4483 are about 2 times younger than those in VII Zw 403 and UGCA 290. We cannot exclude however the possibility that some of these differences are also caused by metallicity effects. Among this group, VII Zw 403 has the largest age and/or stellar metallicity because its AGB stars are the least luminous.

With our adopted larger distance of 15.8 Mpc, an appreciable number of red stars, most likely AGB stars, with absolute  $I$  magnitude of  $\sim -6$  mag or brighter can be seen in the CMD of I Zw 18. They are  $\sim 1$  mag brighter than in UGC 4483. These stars are also bluer than in other galaxies, as expected from the low metallicity of I Zw 18. They were first detected and analyzed by Aloisi et al. (1999) who concluded that they have ages of at least 1 Gyr. They are also present in the *HST* NICMOS near-infrared CMD of I Zw 18 by Östlin (2000) who derived ages of up to 5 Gyr using Padua theoretical isochrones with  $Z = 0.0004$  (Bertelli et al. 1994). Given the uncertainties of these isochrones as discussed in section 3, these ages are probably overestimates and are not likely to exceed 1 Gyr. Support for a relatively small age of the AGB stars in I Zw 18 comes from their spatial distribution shown in Fig. 15. Filled circles denote red stars with  $(V - I) \geq 1.0$  mag and open circles all other stars detected in the PC image of I Zw 18. The locations of the bright star-forming NW and SE regions are shown by crosses. Aloisi et al. (1999) first noted that the red AGB stars are located in the south-eastern part of the galaxy. We confirm this result. We also note that these AGB stars are detected in the same crowded regions where bluer and younger stars are present. Such a distribution is very different from that seen in UGC 4483, VII Zw 403 (Lynds et al. 1998; Schulte-Ladbeck et al. 1998), UGCA 290 (Crone et al. 2000) and NGC 2366 (Thuan & Izotov 2001) where the RGB and AGB stars are spread out over significantly larger areas as compared to the younger stars. This difference in spatial distribution may be an indication that AGB stars in I Zw 18 have had no time to diffuse far away from

their origin and hence may be significantly younger than 1 Gyr. The compact distribution of the AGB stars and their conspicuous absence at larger distances in non-crowded regions where they can be more easily detected, also argue against the idea that I Zw 18 possesses an extended low-surface-brightness disk of red stars (Legrand 2000; Kunth & Östlin 2000). Deeper images (by 1–2 mag) of I Zw 18 are required to check for the presence or absence of RGB stars in this BCD and settle the controversy on its age. This will be possible with the future Advanced Camera for Surveys (ADS) to be installed on *HST*.

In conclusion, *HST* observations of nearby galaxies with resolved stellar populations have not revealed ones as young as  $\lesssim 100$  Myr as suggested by Izotov & Thuan (1999) from chemical arguments. However, there is evidence that suggests that some nearby dwarf galaxies, like I Zw 18, SBS 0335–052 and UGC 4483 have ages which are significantly smaller than the age of the Universe ( $\lesssim 2$  Gyr), and in that sense, can be considered as young galaxies.

## 6. Summary

We present a photometric study of the resolved stellar populations in the nearby cometary blue compact dwarf galaxy UGC 4483 based on *Hubble Space Telescope* WFPC2 *V* and *I* images. The analysis of the color-magnitude diagram (CMD) for this galaxy have led us to the following conclusions:

1. The CMD of UGC 4483 is populated by the stars with different ages including the youngest hydrogen-burning main-sequence stars, evolved massive stars with core helium burning (blue-loop stars and red supergiants), and older red giants and asymptotic giant helium-shell burning stars. Hence, there was continuous star formation in UGC 4483 during a long period, for at least the last 2 Gyr.
2. From the observed *I* magnitude of the tip of the red giant branch (TRGB) of  $23.65 \pm 0.10$  mag, we derive a distance modulus  $(m - M) = 27.63 \pm 0.11$  corresponding to a distance of  $3.4 \pm 0.2$  Mpc and suggesting that UGC 4483 is a member of the M81 group of galaxies.
3. The  $(V - I)$  color of the red giant stars in UGC 4483 is comparatively very blue, with a TRGB  $(V - I) = 1.3$  mag implying a very low metallicity ( $[\text{Fe}/\text{H}] \sim -2.4$ ) and/or a young age of the RGB stars. We argue for a young age of  $\sim 2$  Gyr.
4. The AGB stars in UGC 4483 are significantly brighter than those observed in other dwarf galaxies with similar metallicities. They are, for example,  $\sim 0.3$  mag brighter than those seen in the BCDs VII Zw 403 and UGCA 290. Assuming the stars have the same metallicity as the ionized gas, the higher luminosities suggest that the AGB stars in UGC

4483 are about a factor of 2 younger than those in VII Zw 403 and UGCA 290.

5. We do not find evidence for stellar populations older than 2 Gyr in UGC 4483, although our data is not deep enough to detect the indicators of older stellar populations such as red giant clump and horizontal-branch stars. Comparison of the stellar populations of UGC 4483 with those in other nearby dwarf galaxies suggests that it is likely to be one of the youngest among the BCDs and dwarf irregular galaxies with detected RGB and AGB stars. Alternatively, the differences in the CMD of UGC 4483 can also be explained by an abnormally low metallicity of the stars in the BCD,  $[Fe/H] = -2.4$ , comparable to the most metal-deficient globular cluster stars.

Y.I.I. and T.X.T. are grateful for the partial financial support of NSF grant AST-96-16863. T.X.T. has also been supported by HST-GO-08769.01-A grant. Y.I.I. thanks the hospitality of the Astronomy Department of the University of Virginia. We thank Márcio Catelan and Robert Rood for useful discussions.

## REFERENCES

Aloisi, A., Tosi, M., & Greggio, L. 1999, AJ, 118, 302

Bertelli, G., Bressan, A., Fagotto, F., & Nasi, E. 1994, A&AS, 106, 275

Cole, A. A., et al. 1999, AJ, 118, 1657

Crone, M. M., Schulte-Ladbeck, R. E., Hopp, U., & Greggio, L. 2000, ApJ, 545, L31

Da Costa, G. S., & Armandroff, T. E. 1990, AJ, 100, 162

Dohm-Palmer, R. C., et al. 1997a, AJ, 114, 2514

Dohm-Palmer, R. C., et al. 1997b, AJ, 114, 2527

Dolphin, A. E. 2000a, PASP, 112, 1397

———. 2000b, ApJ, 531, 804

Dolphin, A. E., et al. 2001, MNRAS, 324, 249

Gallagher, J. S., et al. 1998, AJ, 115, 1869

Girardi, L., Bressan, A., Bertelli, G., & Chiosi, C. 2000, A&AS, 141, 371

Guseva, N. G., Izotov, Y. I., Papaderos, P., Chaffee, F. H., Foltz, C. B., Green, R. F., Thuan, T. X., Fricke, K. J., & Noeske, K. G. 2001, A&A, 378, 756

Harris, W. E. 1996, AJ, 112, 1487

Henry, R. C. B., Edmunds, M. G., & Köppen, J. 2000, ApJ, 541, 660

Holtzman, J., et al. 1995a, PASP, 107, 156

Holtzman, J., et al. 1995b, PASP, 107, 1065

Hunter, D. A., & Thronson, H. A., Jr. 1995, ApJ, 452, 238

Izotov, Y. I., & Thuan, T. X. 1999, ApJ, 511, 639

Izotov, Y. I., Thuan, T. X., & Lipovetsky, V. A. 1994, ApJ, 435, 647

Kunth, D., & Östlin, G. 2000, A&A Rev., 10, 1

Landolt, A. U. 1992, AJ, 104, 336

Lee, M. G., Freedman, W. L., & Madore, B. F. 1993, ApJ, 417, 553

Legrand, F. 2000, A&A, 354, 504

Lejeune, T., & Schaerer, D. 2001, A&A, 366, 538

Loose, H.-H., & Thuan, T. X. 1986, in Star Forming Dwarf Galaxies and Related Objects, ed. D. Kunth, T. X. Thuan & J. T. T. Van (Gif-sur-Yvette: Editions Frontières), 73

Lynds, R., Tolstoy, E., O’Neil, E. J., Jr., & Hunter, D. A. 1998, AJ, 116, 146

Marigo, P. 2001, A&A, 370, 194

Noeske, K. G., Guseva, N. G., Fricke, K. J., Izotov, Y. I., Papaderos, P., & Thuan, T. X. 2000, A&A, 361, 33

Östlin, G. 2000, ApJ, 535, L99

Papaderos, P., Izotov, Y. I., Noeske, K. G., Thuan, T. X., & Fricke, K. J. 2001, in Dwarf Galaxies and their Environment, eds. K.S. de Boer, R.-J. Dettmar & U. Klein, Shaker Verlag, p. 111

Pilyugin, L. S. 1999, A&A, 346, 428

Roy, J.-R., & Kunth, D. 1995, A&A, 294, 432

Schaerer, D., & Vacca, W. D. 1998, ApJ, 497, 618

Schlegel, D. J., Finkbeiner, D. P., & Davis, M. 1998, ApJ, 500, 525

Schulte-Ladbeck, R. E., Crone, M. M., & Hopp, U. 1998, ApJ, 493, L23

Skillman, E. D. 1991, PASP, 103, 919

Skillman, E. D., Terlevich, R. J., Kennicutt, R. C., Jr., Garnett, D. R., & Terlevich, E. 1994, ApJ, 431, 172

Tantalo, R., Chiosi, C., Bressan, A., & Fagotto, F. 1996, A&A, 311, 361

Thuan, T. X., & Izotov, Y. I. 2001, in preparation

Thuan, T. X., Izotov, Y. I., & Foltz, C. B. 1999, ApJ, 525, 105

Thuan, T. X., Izotov, Y. I., & Lipovetsky, V. A. 1995, ApJ, 445, 108

———. 1997, ApJ, 477, 661

Thuan, T. X., & Seitzer, P. O. 1979, ApJ, 231, 327

Tikhonov, N. A., & Karachentsev, I. D. 1993, A&A, 275, 39

Tolstoy, E., et al. 1998, AJ, 116, 1244

Wyder, T. K., Hodge, P. W., & Zucker, D. B. 2000, PASP, 112, 1162

Table 1. Photometry completeness<sup>a</sup>

Mag.	PC		WF4	
	F555W	F814W	F555W	F814W
23 – 24	100.0	100.0	100.0	100.0
24 – 25	96.4 ± 5.0	91.3 ± 7.1	93.3 ± 14.9	84.4 ± 14.9
25 – 26	80.6 ± 9.0	78.5 ± 12.4	80.0 ± 7.5	72.4 ± 9.2
26 – 27	69.5 ± 3.5	54.4 ± 7.5	66.9 ± 10.4	44.8 ± 8.4
27 – 28	40.5 ± 5.2	15.1 ± 7.2	44.2 ± 12.1	6.7 ± 9.4
28 – 29	11.2 ± 6.6	...	12.2 ± 6.0	...

<sup>a</sup>expressed in percentage of recovered stars.

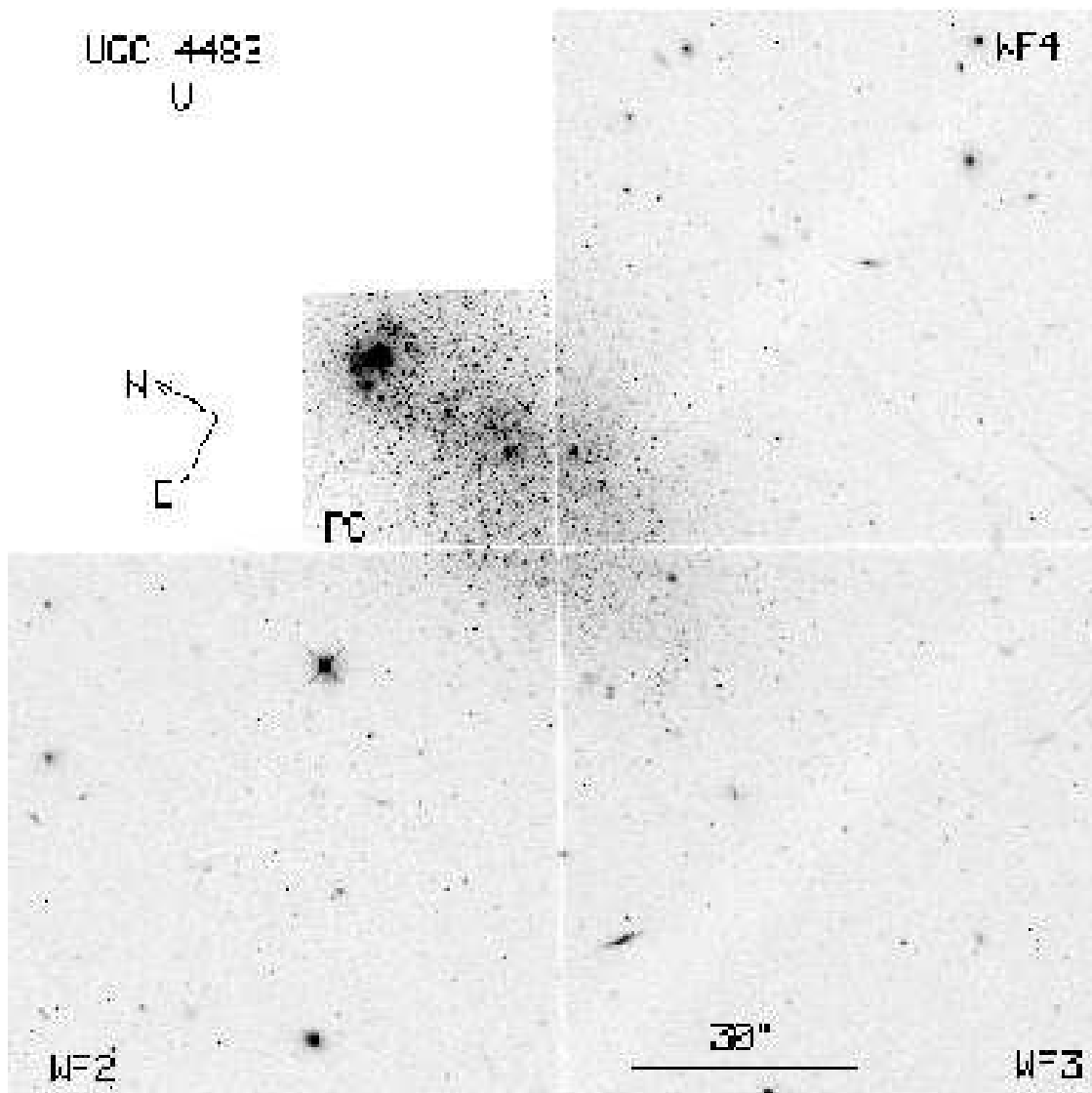


Fig. 1.— *HST V* mosaic image of UGC 4483. The regions of the ongoing and recent star formation are at the northern edge of the galaxy in the PC frame. Many background galaxies are also seen suggesting that UGC 4483 is projected onto a distant cluster of galaxies.

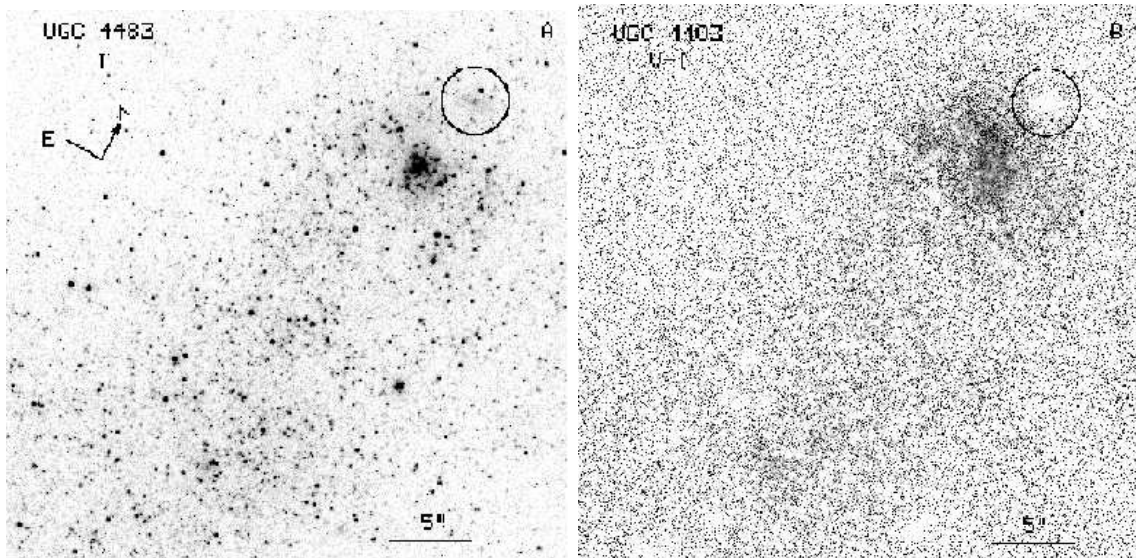


Fig. 2.— PC  $I$  (a) and  $V - I$  (b) images. In the  $V - I$  image blue is black and red is white. Enclosed within the circle is a red regularly shaped background galaxy. The brightness distribution is clumpy implying that differential dust extinction is likely to be present.

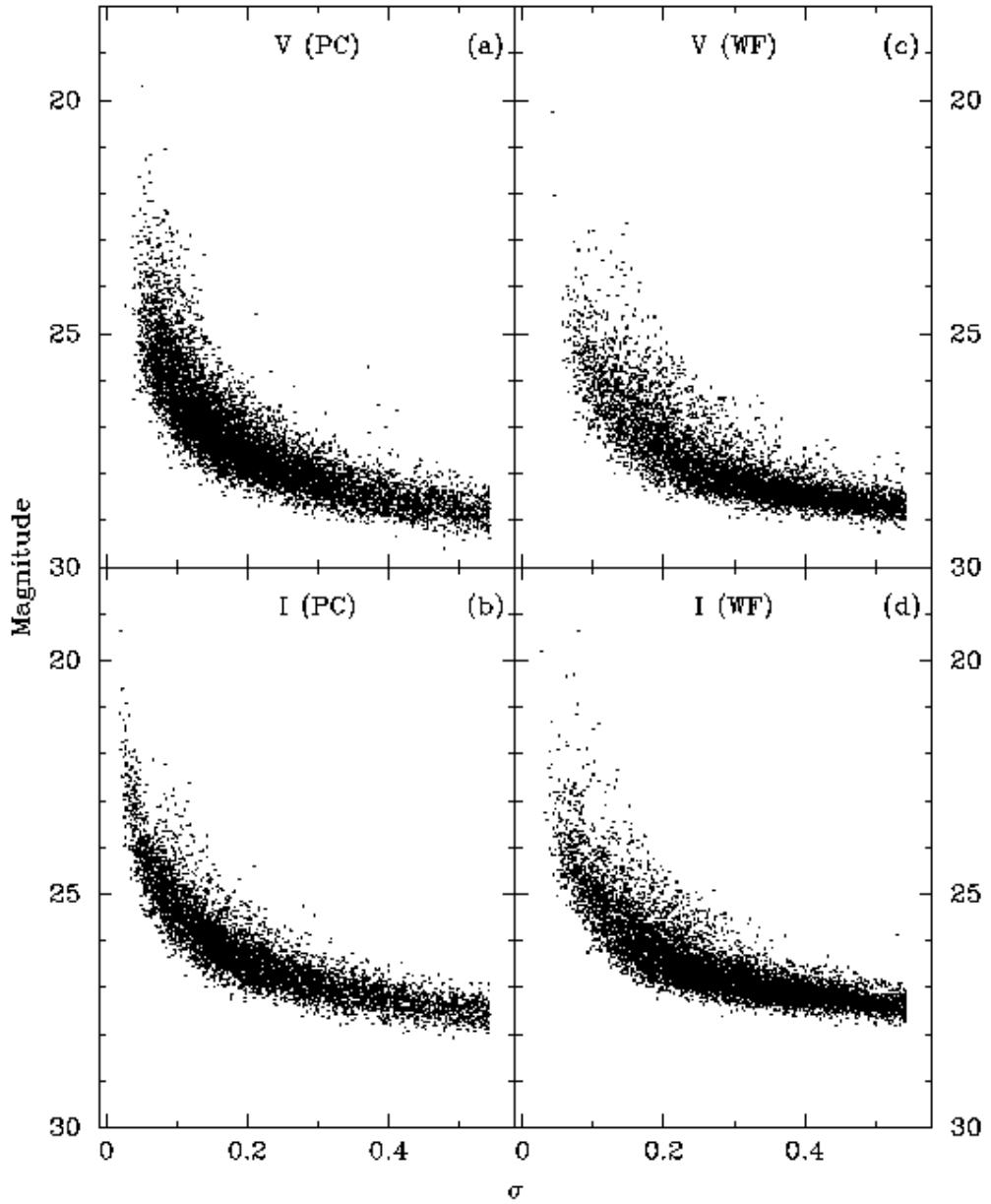


Fig. 3.— Photometric error  $\sigma$  as a function of apparent magnitude in both  $V$  and  $I$  images for the PC frame (a and b) and for the combined WF2,WF3,WF4 frames (c and d). The  $V$  photometry is  $\sim 1$  mag deeper than the  $I$  photometry, going down to a limiting magnitude of 29 mag.

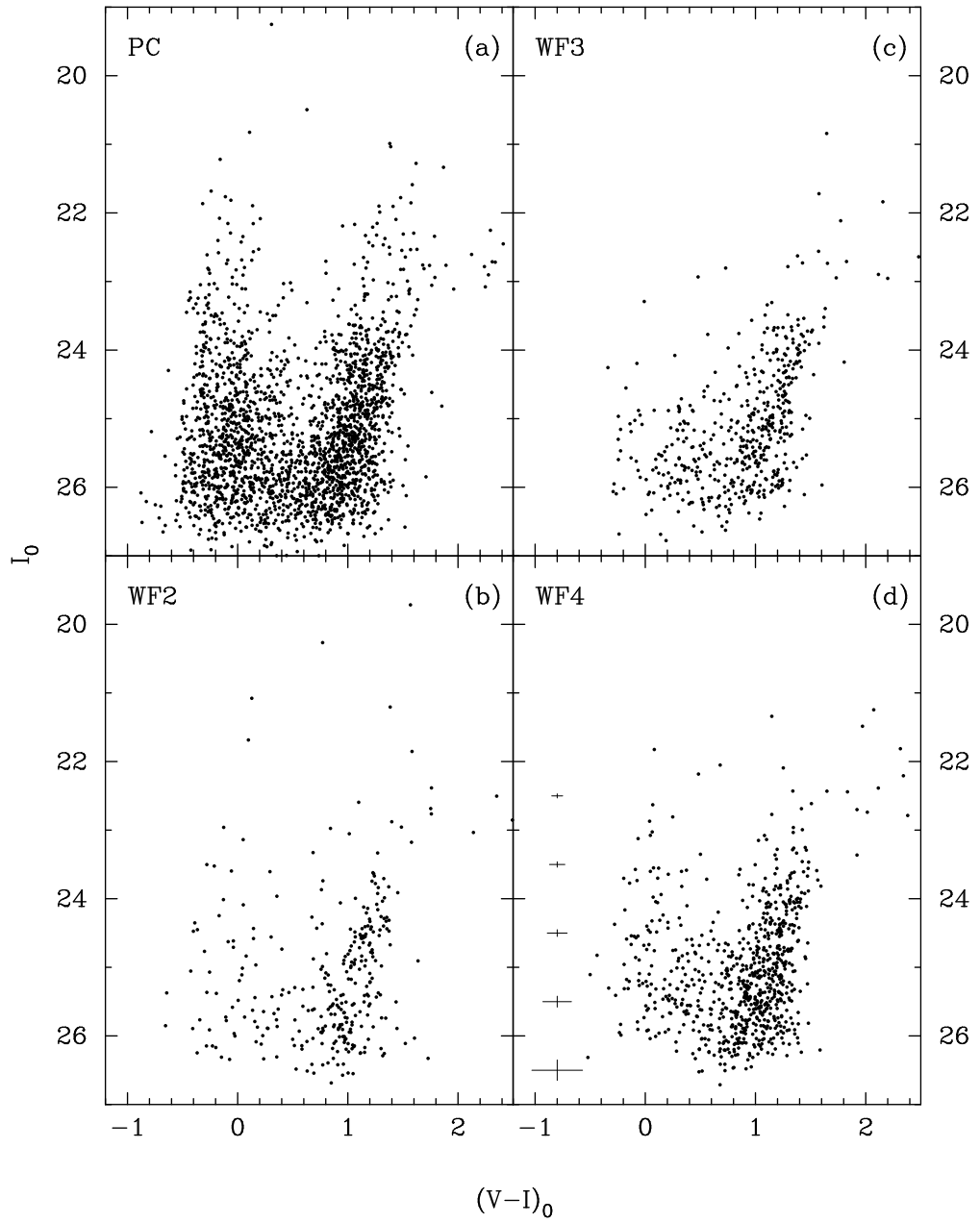


Fig. 4.—  $(V - I)_0$  vs  $I_0$  color-magnitude diagrams in each of the PC and WF frames. The observed magnitudes and colors are transformed to the standard Johnson-Cousin  $VI$  photometric system and corrected for aperture and extinction adopting  $E(B - V) = 0.11$  mag. The photometric errors are shown by vertical and horizontal bars in panel (d).

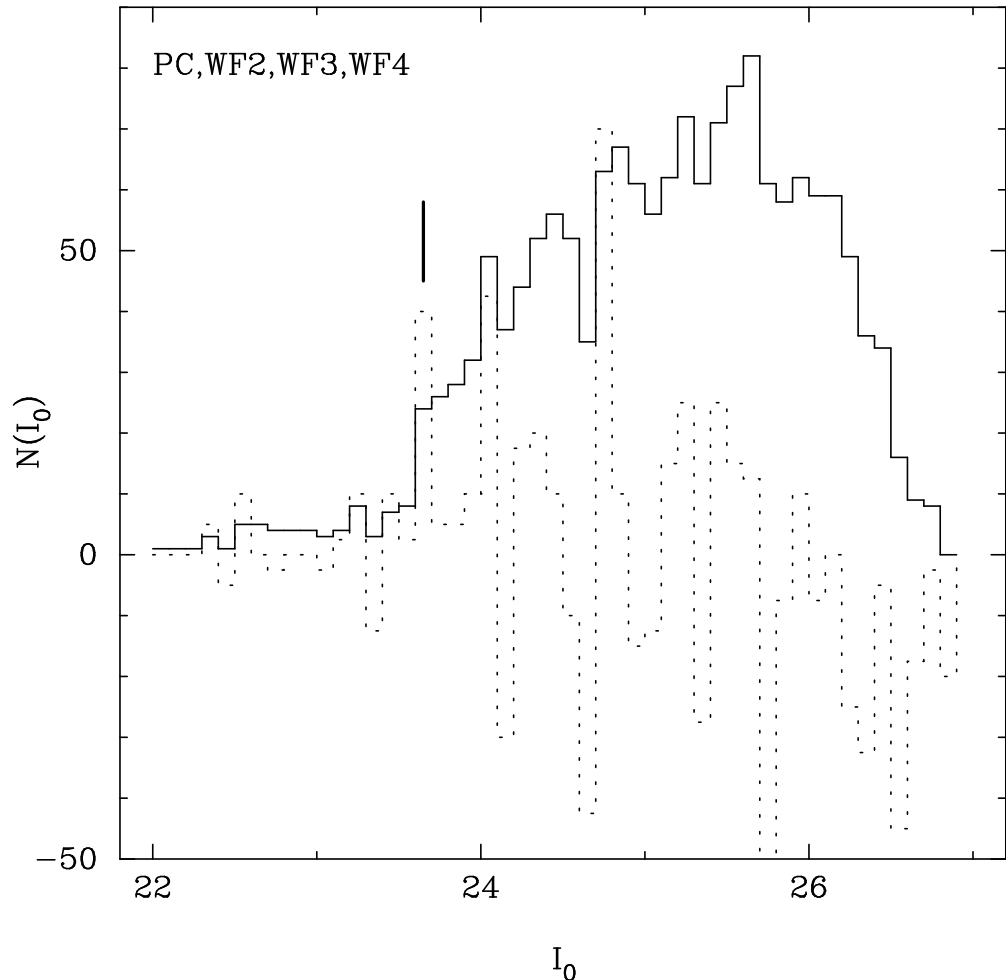


Fig. 5.— Distribution of red giant branch stars as a function of apparent  $I_0$  magnitude (solid line) in the combined PC, WF2, WF3, WF4 frames. The dotted line shows the derivative of the RGB star number distribution. The location of the RGB tip is marked by vertical line and corresponds to  $I_0 = 23.65$  mag.

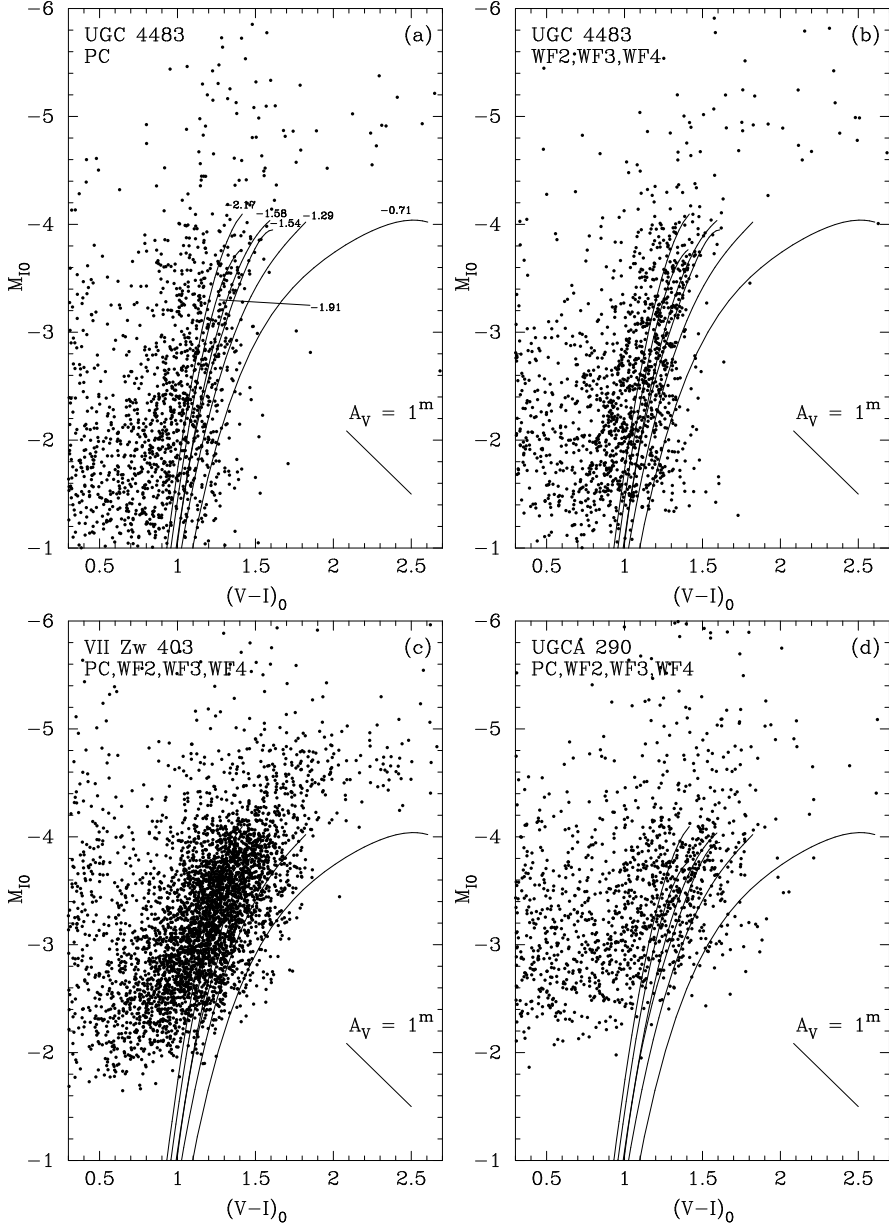


Fig. 6.— Absolute magnitude  $M_{I0}$  vs  $(V - I)_0$  diagram of the RGB stars in UGC 4483 for (a) the PC frame and (b) the combined WF2, WF3, WF4 frames. The adopted distance modulus is  $m - M = 27.63$ . Magnitudes and colors are corrected for Galactic extinction with  $A_V = 0.11$  mag. In (c) and (d) are given similar plots for the BCDs VII Zw 403 and UGCA 290. The distance modulus and extinction correction are taken from Lynds et al. (1998) for VII Zw 403 and Crone et al. (2000) for UGCA 290. The superimposed solid lines are, from left to right, the observed isochrones arranged in order of increasing metallicity of the globular clusters M15 ( $[\text{Fe}/\text{H}] = -2.17$ ), NGC 6397 ( $-1.91$ ), M2 ( $-1.58$ ), NGC 6752 ( $-1.54$ ), NGC 1851 ( $-1.29$ ) and 47 Tuc ( $-0.71$ ) (Da Costa & Armandroff 1990). The metallicity labels are given in panel (a).

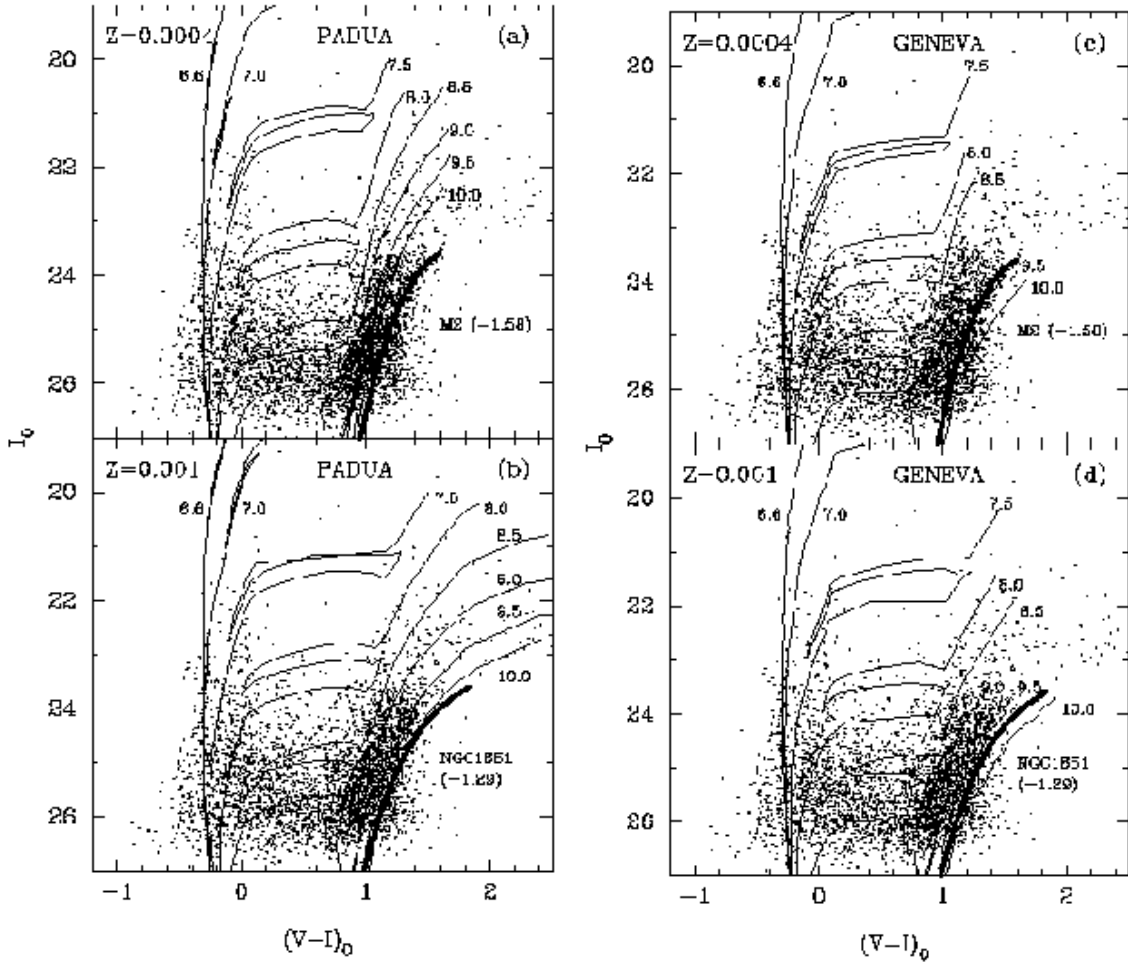


Fig. 7.— Comparison of theoretical isochrones (thin lines) with observed ones of two globular clusters (M2 and NGC 1851) with matching metallicities (thick lines) for two sets of models: Padua models with  $Z = 0.0004$  (a) and  $Z = 0.001$  (b) (Bertelli et al. 1994), and Geneva models with  $Z = 0.0004$  (c) and  $Z = 0.001$  (d) (Lejeune & Schaerer 2001). Each theoretical isochrone is labeled by the logarithm of the age in year. The isochrones are overplotted on the CMD of UGC 4483. Only the Padua model with  $Z = 0.001$  fits reasonably well the isochrone for the globular cluster NGC 1851 (b). The Padua model with  $Z = 0.0004$  (a) cannot fit the reddest part of the RGB in UGC 4483.

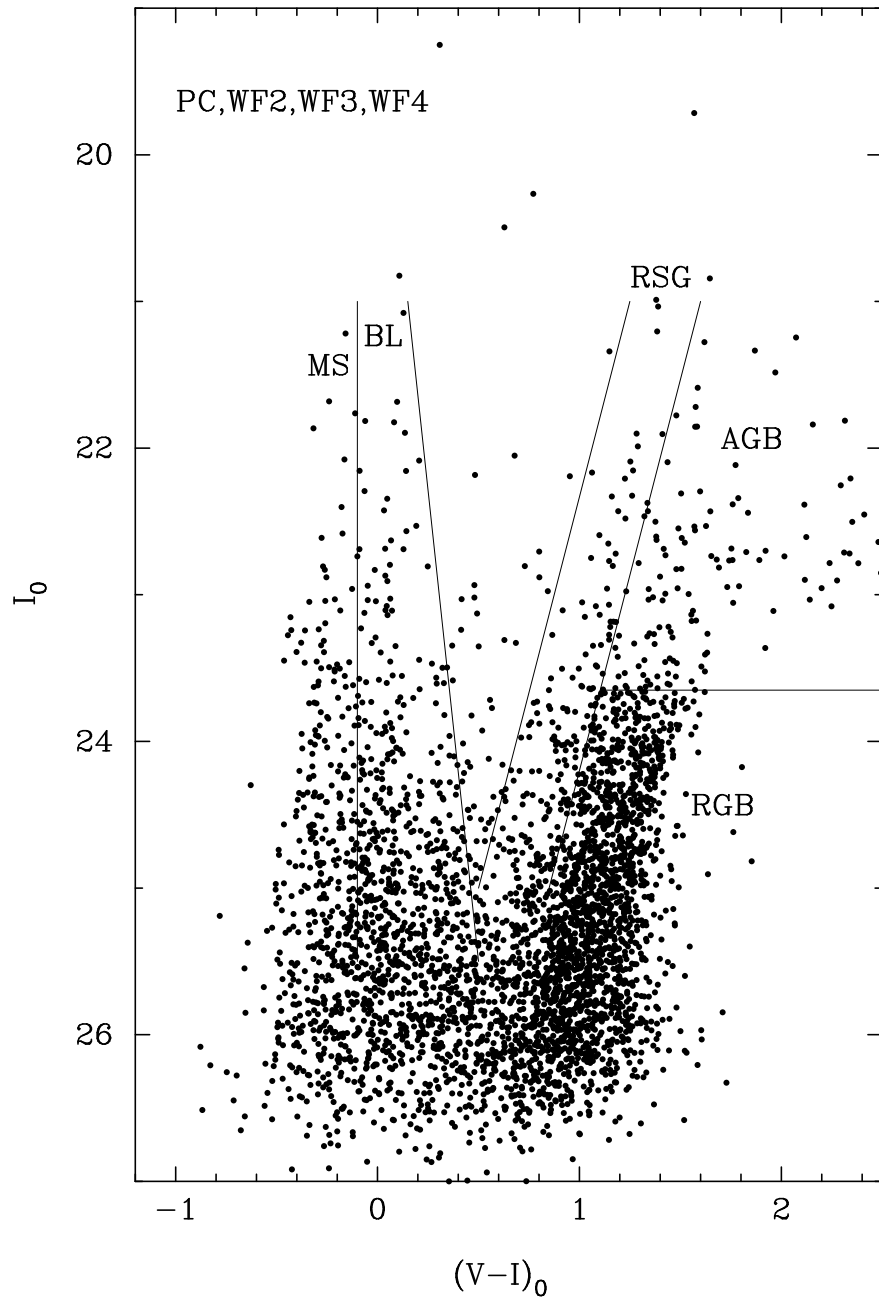


Fig. 8.— Combined CMD of UGC 4483 overplotted by lines showing the locations of main-sequence (MS), blue loop (BL), red supergiant (RSG), red giant (RGB) and asymptotic giant branch (AGB) stars.

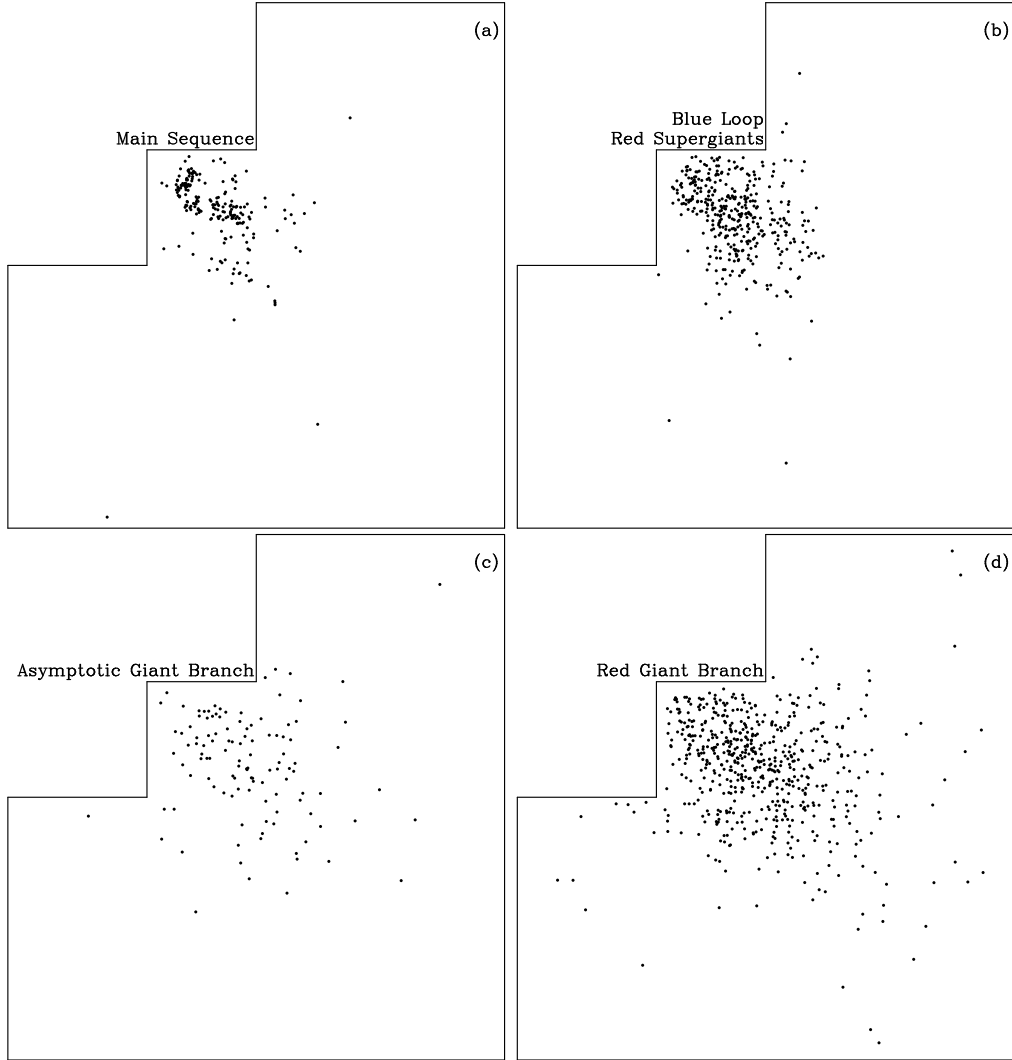


Fig. 9.— Spatial distribution of the (a) main-sequence, (b) blue loop and red supergiant, (c) asymptotic giant branch and (d) red giant branch stars in UGC 4483. The main sequence stars show a clumpy distribution and are concentrated mainly in the PC frame. Stars with progressively increasing ages [(b) to (d)] are distributed more smoothly and occupy successively larger volumes in the galaxy. The WFPC2 camera covers 160" on a side.

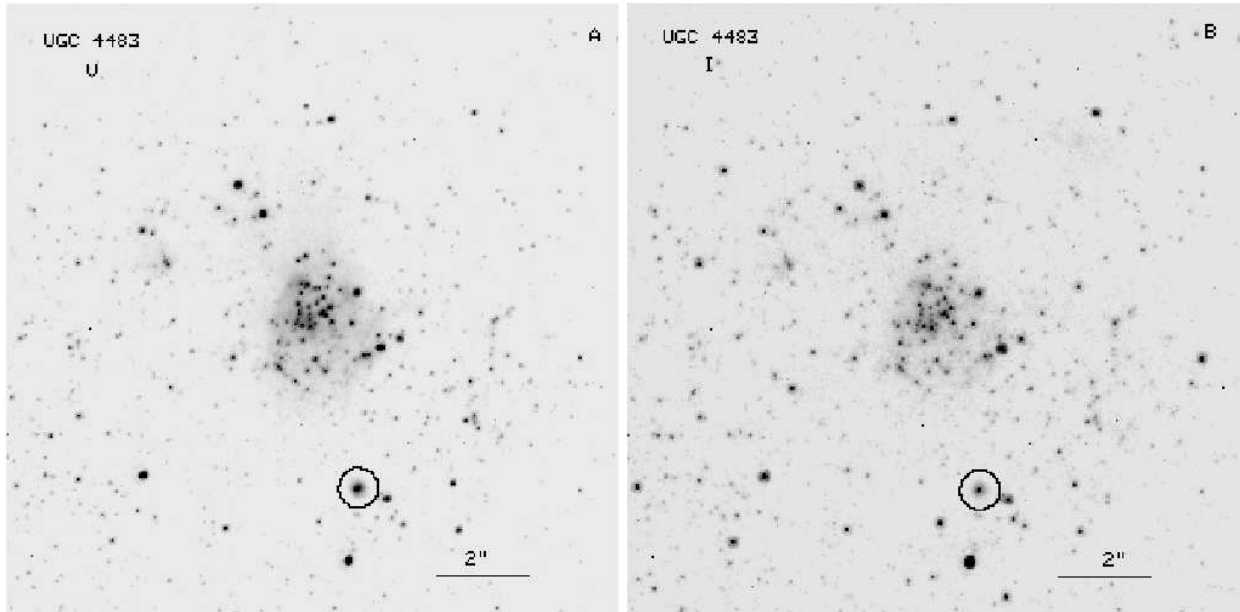


Fig. 10.—Area of the PC image in  $V$  (a) and  $I$  (b) which contains the brightest and youngest stellar cluster. Ionized gas is visible around the cluster. The compact blue object marked by the circle is an H II region associated with a single hot, presumably of the Wolf-Rayet type. The orientation is the same as in Figure 2.

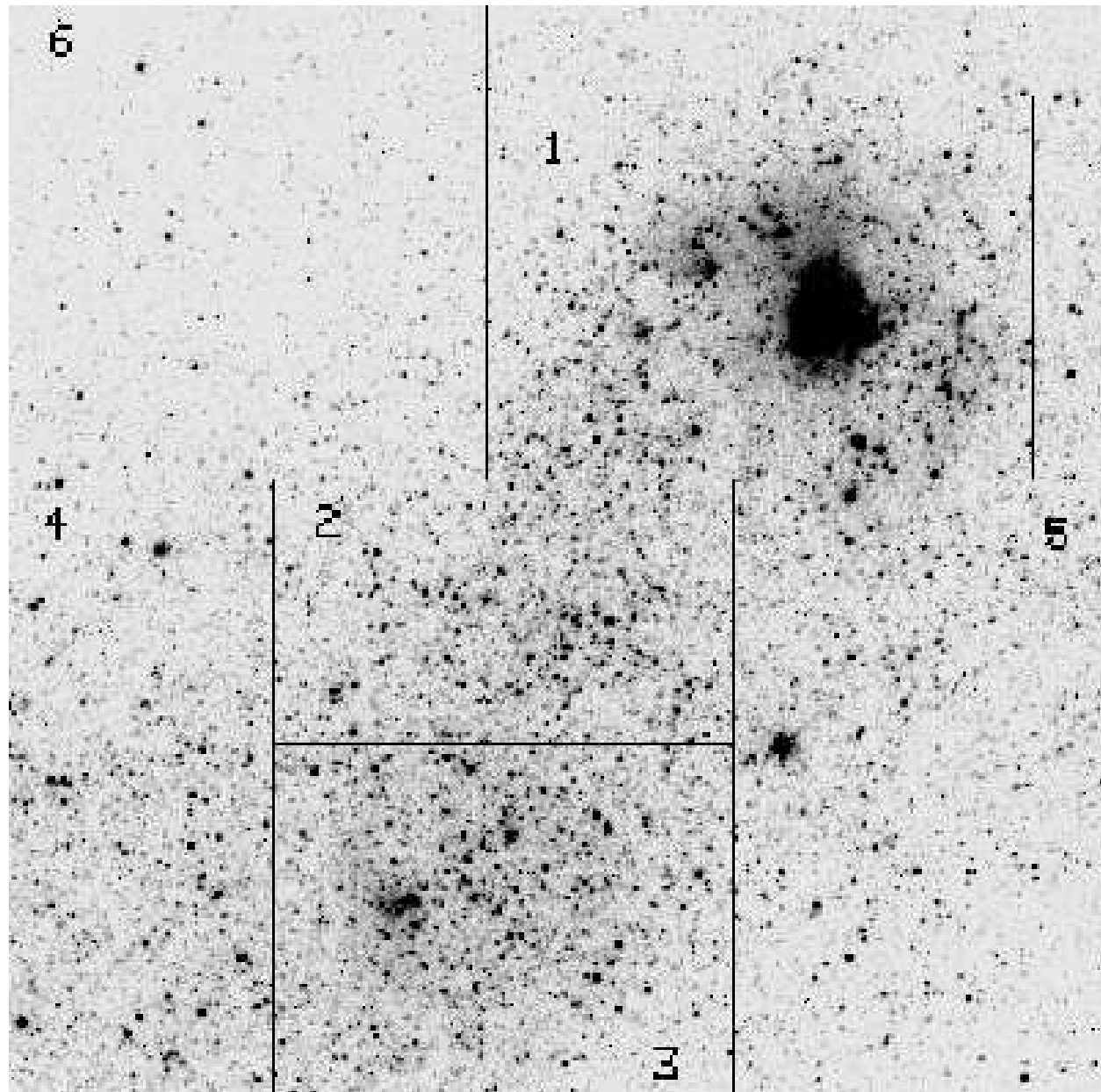


Fig. 11.— PC V image of UGC 4483 divided into 6 different regions for CMD analysis of the stellar populations (see Fig. 12). The image is 36''.8 on a side. The orientation is the same as in Figure 2.

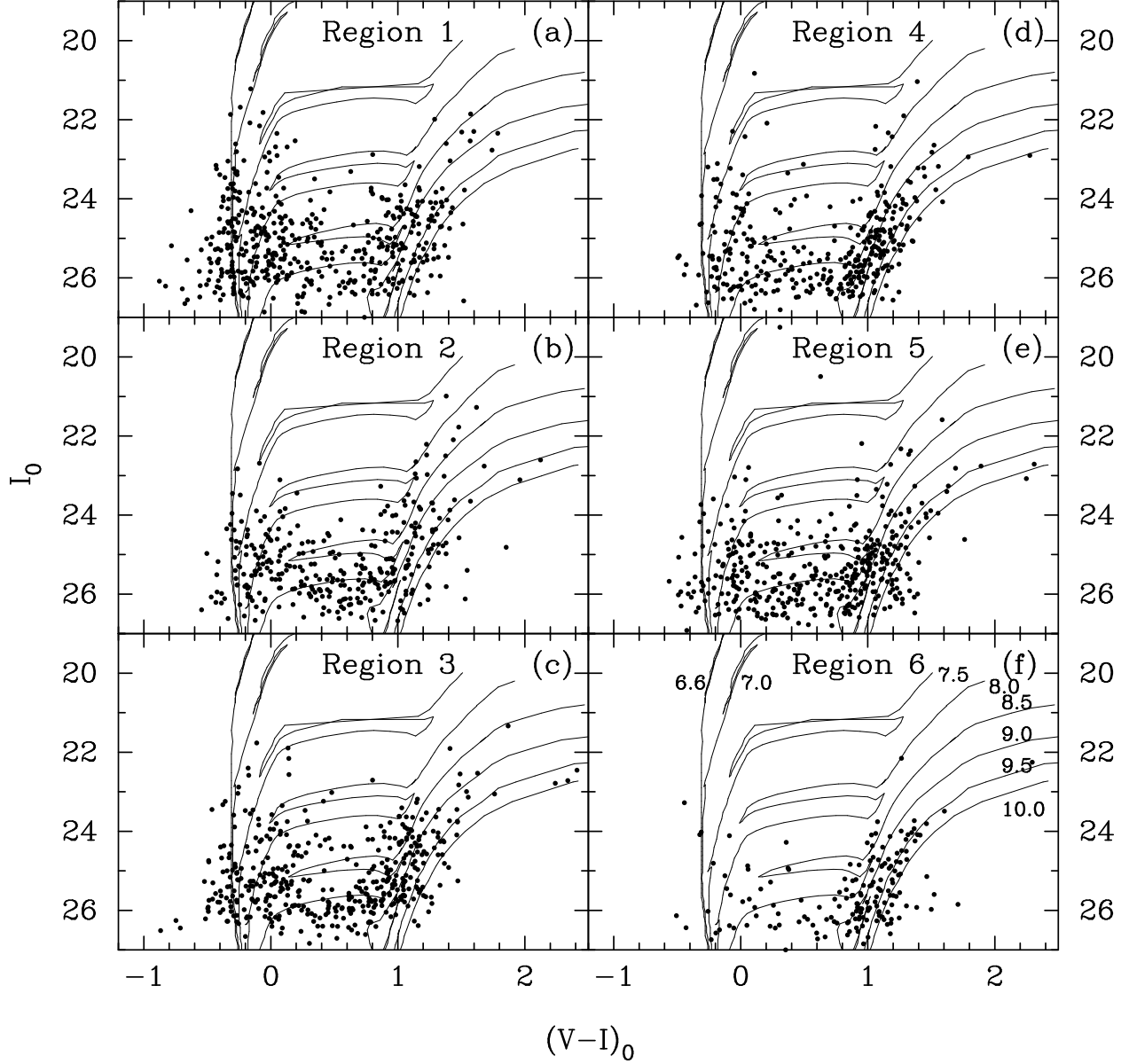


Fig. 12.—  $(V - I)_0$  vs  $I_0$  CMDs for the 6 regions of UGC 4483 shown in Fig. 11. Superimposed are theoretical isochrones for a heavy element mass fraction  $Z = 0.001$  (Bertelli et al. 1994). The logarithms of the ages in years for each isochrone are shown in (f). Populations of different ages are present in regions 1 – 5 suggesting continuous star formation during the last  $\sim 2$  Gyr. Region 6 is populated only by a relatively old stellar population of 300 Myr – 2 Gyr.

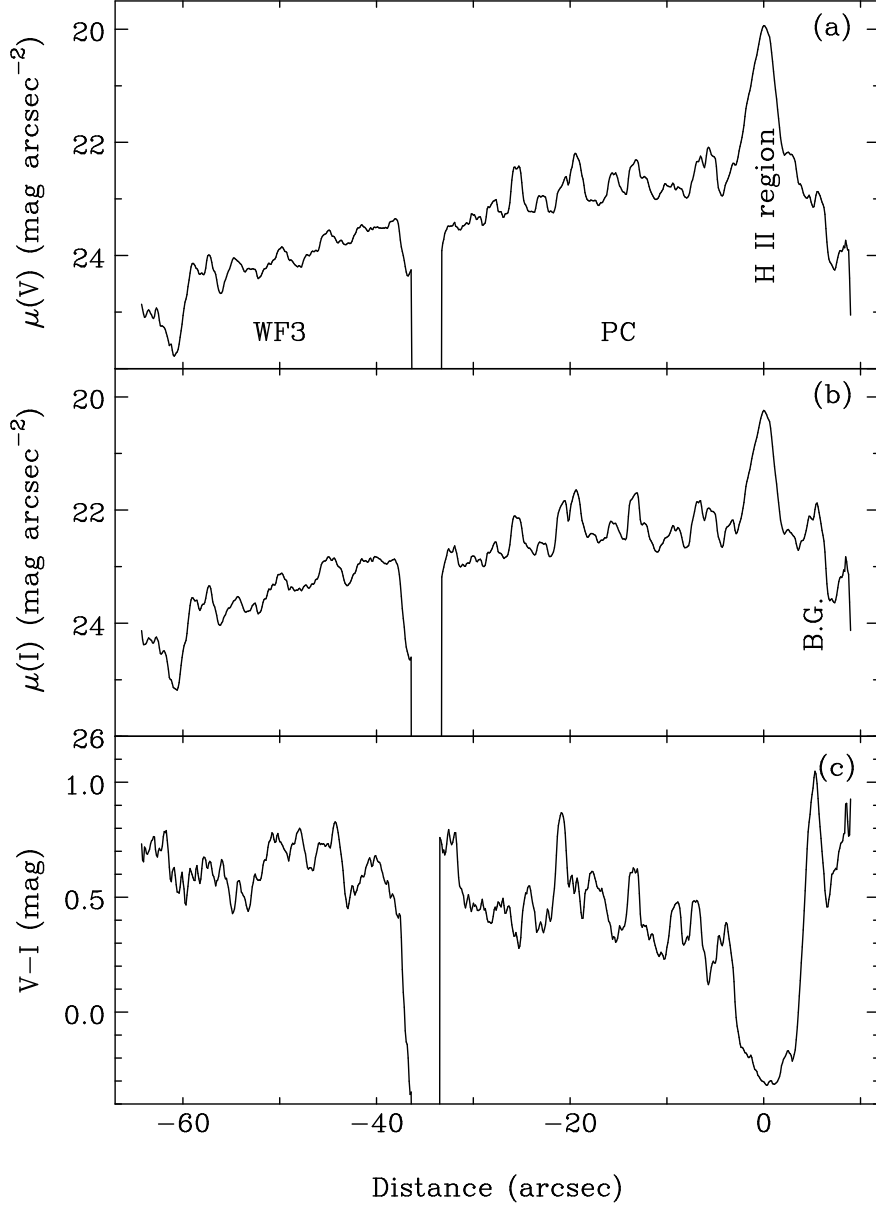


Fig. 13.—  $V$  (a) and  $I$  (b) surface-brightness and ( $V - I$ ) color (c) profiles along the major axis of UGC 4483 (along the diagonals of the PC and WF3 frames) in a 2 arcsec wide strip. The distributions are smoothed by a 11 point box-car. The gap in the profiles at  $\sim -35''$  is caused by the lack of signal at the boundaries of the CCD chips (Fig. 1). The origin is taken to be at the location of the supergiant H II region (marked in panel (a)). The red background galaxy seen in Fig. 2 is marked as B.G. in panel (b).

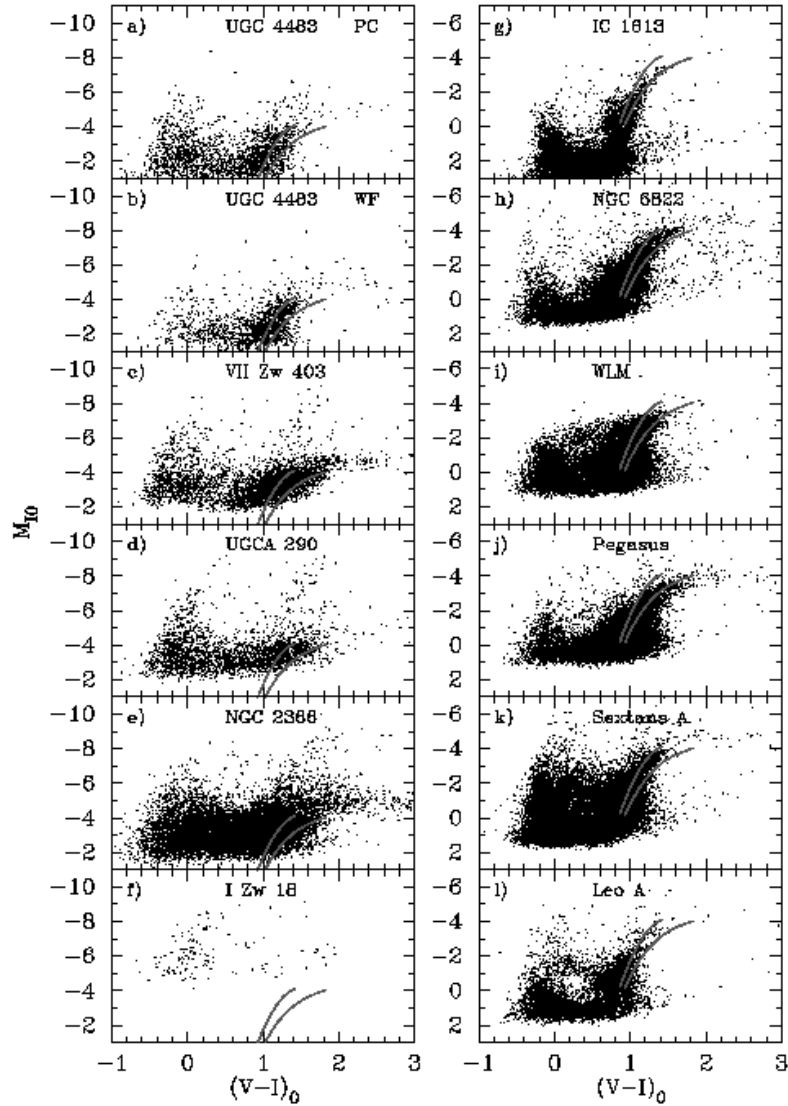


Fig. 14.— CMDs for 5 blue compact dwarf and irregular galaxies outside the Local Group (panels a to f) and 6 Local Group irregular galaxies (panels g to l) based on *HST* WFPC2 images. For comparison are shown in each panel the isochrones of the globular clusters M15 ( $[\text{Fe}/\text{H}] = -2.17$ ) (left solid line) and NGC 1851 ( $[\text{Fe}/\text{H}] = -1.29$ ) (right solid line) (Da Costa & Armandroff 1990).

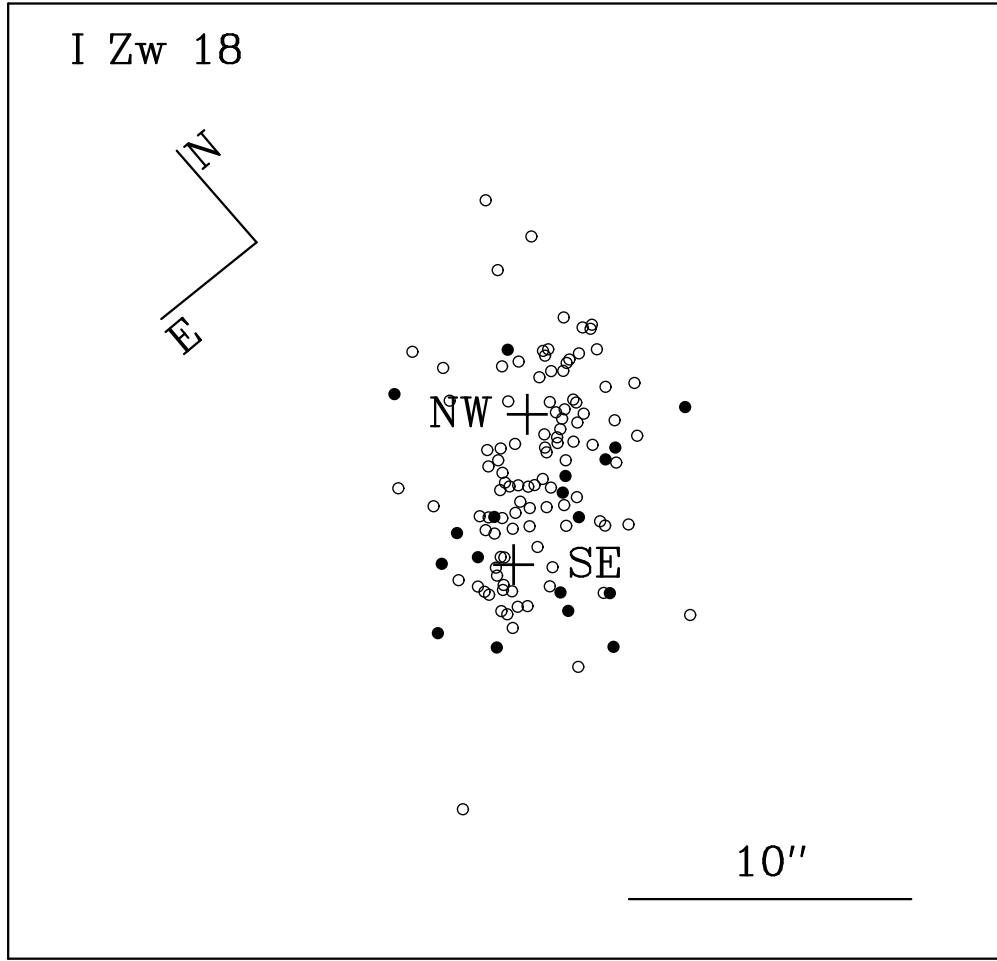


Fig. 15.— Spatial distribution of evolved red ( $(V - I) \geq 1.0$  mag) AGB stars (filled circles) and younger bluer ( $(V - I) < 1.0$  mag) stars (open circles) in the BCD I Zw 18. The NW and SE star-forming regions are marked by crosses. Note the relatively compact distribution of the AGB stars around the SE region, as compared to their more spread-out distribution in other dwarf galaxies (see Fig. 9)